Late Cenozoic extension in SW Bulgaria: a synthesis

ROB WESTAWAY

Faculty of Mathematics and Computing, The Open University, Eldon House, Gosforth, Newcastle upon Tyne NE3 3PW, UK (e-mail: r.w.c.westaway@ncl.ac.uk)

Also at: School of Civil Engineering and Geosciences, University of Newcastle-upon-Tyne NE1 7RU, UK

Abstract: Southwest Bulgaria forms the northern margin of the Aegean extensional province. Since the Early Pliocene (*c.* 4 Ma), this region has accommodated southward or SSE extension at several millimetres per year, superimposed on *c.* 400 m of post-Early Pliocene regional uplift. This sense of deformation superseded earlier extension, oriented ENE–WSW, which is estimated to have begun in the early Late Miocene (*c.* 10–9 Ma) and lasted until *c.* 4 Ma. The regional topography is dominated by NNW–SSE-striking grabens and normal fault escarpments, relics from this time. Normal faults that are now active cut across these older structures, although in some localities normal faults that were oriented obliquely to the earlier extension have remained active, also oblique to the modern extension sense. It is suggested that this present phase of extension relates to the modern sense of deformation throughout the Aegean region and to the modern geometry of the North Anatolian Fault Zone (NAFZ), which is independently inferred to have existed since *c.* 4 Ma. The earlier ENE–WSW extension is inferred to have involved two phases, the first predating the NAFZ and the second synkinematic with its initial phase of slip during *c.* 7–4 Ma, when its geometry and the overall sense of deformation in the Aegean region were different from at present. Some previous studies have inferred that SW Bulgaria experienced large-scale extension on low-angle normal faults in the Mid-Miocene or earlier. However, the limited evidence in support of this view is open to other interpretations, and after due consideration can be discounted.

Southwest Bulgaria forms the northern part of the Aegean extensional province (Figs 1 and 2), but has featured in the international literature much less than other parts of this region, such as central Greece and western Turkey. This study will concentrate on two Neogene terrestrial depocentres in SW Bulgaria with general NNW–SSE trends, which are now drained by the Struma (Strimon) and Mesta (Nestos) rivers, separated by the Rila and Pirin massifs (Fig. 2). This region thus resembles western Turkey, with subparallel Late Cenozoic depocentres transecting ancient metamorphic massifs (analogous to the Alaşehir and Büyük Menderes grabens and central Menderes Massif; Fig. 1a). This study will thus summarize information regarding timings, rates, senses and amounts of extension in SW Bulgaria, and where possible will draw analogies with western Turkey.

One difference concerns topography. The land surface reaches 2925 and 2915 m in the Rila and Pirin massifs (Fig. 2), *c.* 1 km above the highest points in the Menderes Massif. These high altitudes mean that, unlike most mountain ranges in western Turkey (see Erinç 1978; Demir *et al.* 2004), Rila and Pirin were extensively glaciated during cold stages of the Pleistocene (e.g. Velchev 1995; Zagorchev 1995). Another difference concerns climate. Although southern Bulgaria is barely 100 km from the Aegean coast, the characteristic Mediterranean climate, with hot dry summers and warm wet winters, gives way abruptly northward to a different regime, with maximum rainfall (locally >2000 mm; Furlan 1977) in summer (notably, in June). One consequence of this rainfall seasonality is much more profuse vegetation than in most of western Turkey, limiting field exposures of normal faults and sediments.

One aspect in common between western Turkey and SW Bulgaria is that active normal faulting is superimposed on a background of regional uplift. This idea is well established in Bulgaria (e.g. Zagorchev 1992*a*) but has developed only recently in western Turkey (e.g. Westaway *et al.* 2004). It is thus of interest to compare the uplift histories of the two regions. Another is that investigation of young crustal extension, taken up on initially steep normal faults, has become mixed up in both regions with hypothetical earlier low-angle normal faulting. This association makes it difficult to disentangle the two forms of evidence in some past publications (e.g. that by Burchfiel *et al.* 2000). Although

From: ROBERTSON, A. H. F. & MOUNTRAKIS, D. (eds) 2006. *Tectonic Development of the Eastern Mediterranean Region*. Geological Society, London, Special Publications, **260**, 557–590.
0305-8719/06/$15.00 © The Geological Society of London 2006.

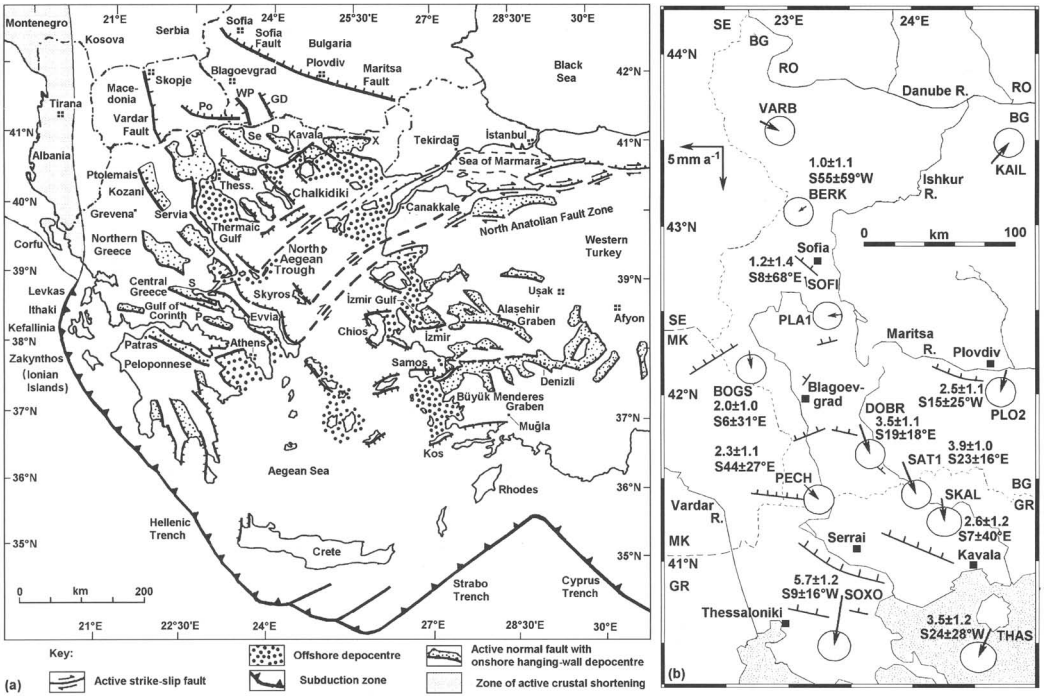

Fig. 1. (**a**) Map of the Aegean extensional province, showing active faulting and related sedimentation, adapted from Westaway (1994, 2002*c*). The right-lateral North Anatolian Fault Zone enters the study region from the NE, its strands terminating against NE-dipping normal fault zones bounding the NE coasts of Evvia and adjacent islands. Thess, Thessaloniki; GD, Po and WP, Gotse Delchev, Podgorie and West Pirin normal faults in SW Bulgaria; D, L, Se and X, Drama, Langadas, Serrai (Serres) and Xanthi grabens in northern Greece; P and S, Parnassos and Sperchios normal faults in central Greece. (**b**) Crustal velocity field across SW Bulgaria, measured by GPS surveys in 1994–1998 (data from Kotzev *et al.*, 2001, fig. 4; McClusky *et al.* 2000), illustrating a gradual increase in southward velocity relative to Eurasia, starting south of point BERK. Kotzev *et al.* (2001) inferred from this dataset that a single notional zone of NW–SE extension at up to *c.* 4 mm a^{-1} transects this region, located between the Vitosha Mountains and the Rila Massif (i.e. south of PLA1 and north of BOGS and PLO2. However, the geological evidence favours more widely distributed southward extension instead.

low-angle normal faulting is mechanically feasible (e.g. Westaway 1999, 2005), to cause the stress field at depth to rotate sufficiently to allow a planar normal fault to form with an initial dip as low as *c.* 30° requires a demanding set of physical conditions, and no-one has ever demonstrated that such conditions have existed in the Late Cenozoic in either Bulgaria or Turkey. Claims regarding low-angle normal faulting in western Turkey have anyway been considered mistaken, because thermochronological evidence of cooling attributed to this process may instead represent erosion (e.g. Westaway 1996, 2006) and because initially steep normal faults may develop low-angle dips by back-tilting (e.g. Bozkurt 2000; Purvis & Robertson 2004). Criticism of the idea of Late Cenozoic low-angle normal faulting in Bulgaria (see Zagorchev 1994, 1998*a*, 2001*b*) has been strident (e.g. Zagorchev 2001*b*).

This study will attempt a synthesis of evidence, regarding both steep and possible low-angle normal faulting, for the Late Cenozoic sedimentary basins in SW Bulgaria. Having summarized the evidence, it will estimate rates and senses of extension and rates of regional uplift and consider the regional significance of this normal faulting.

One difficulty is that the existing literature on SW Bulgaria reports many apparently 'neotectonic' faults, as in Figure 2. However, it is evident that this region has experienced a long and complex deformation history (see Zagorchev 1992*a*, *b*, 2001*a*), and that in addition to young normal faults this map shows faults associated with earlier (?Mid-Miocene) NNW–SSE-directed right-lateral strike-slip and even earlier (?Early Miocene) reverse faulting. Furthermore, many of the faults shown affect only metamorphic

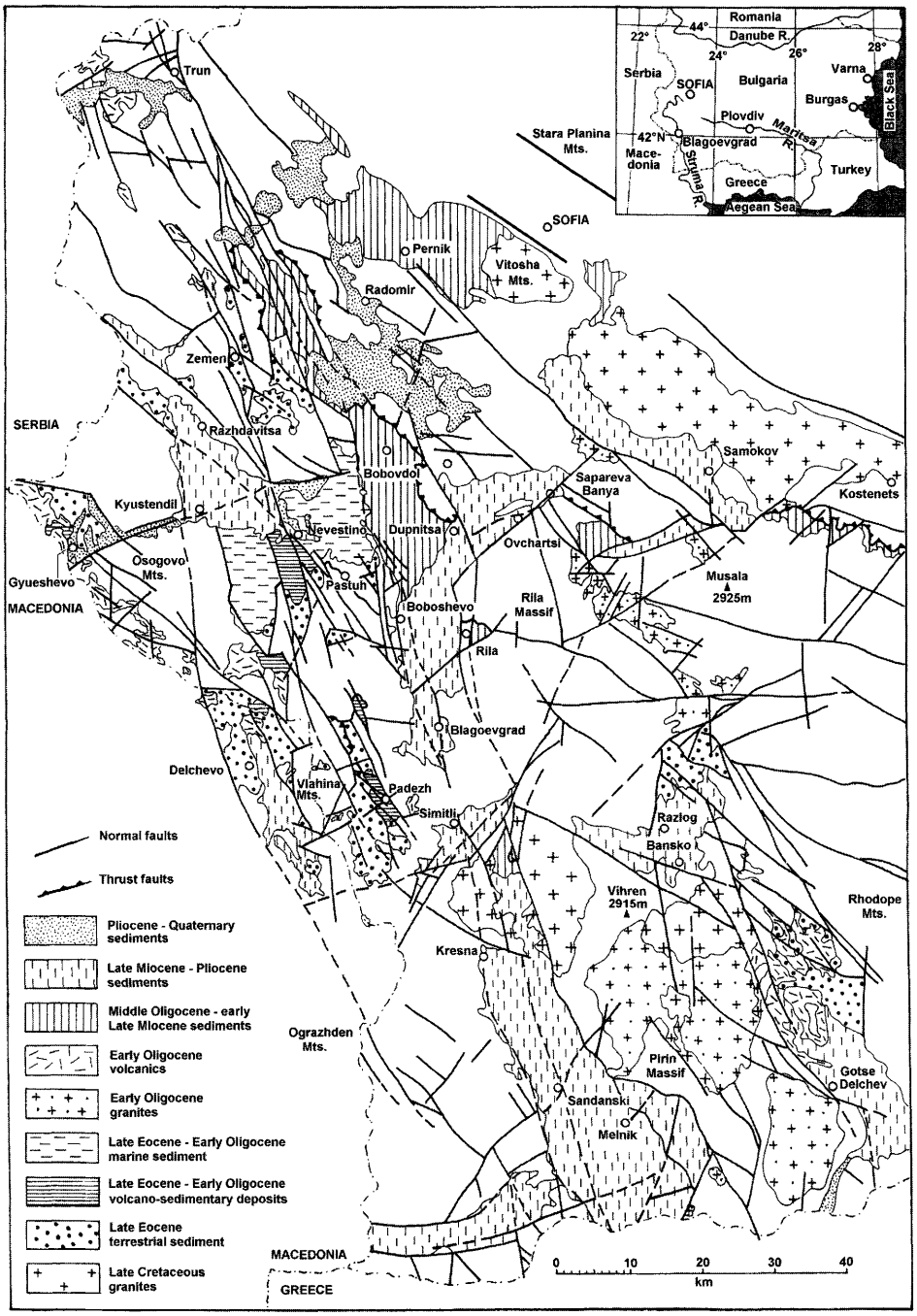

Fig. 2. Map of the present study region in SW Bulgaria, adapted from Zagorchev (1992*b*, fig. 9), who described it as a 'simplified Late Alpine neotectonic map'. Precambrian, Palaeozoic and most Mesozoic rocks are not shaded. The area around Sofia is illustrated only schematically, having been omitted from the map on which this figure is based. The Struma river rises NW of Pernik, from where it flows initially SW through Radomir and Zemen to Kyustendil, then SE to Boboshevo, then SSE past Blagoevgrad, Simitli, Kresna and Sandanski. The Mesta rises south of Kostenets, flowing initially SW to Razlog then SSE past Gotse Delchev. After passing into Greece, both rivers reach the north coast of the Aegean Sea.

basement, and so could be ancient, and others indicate how such old faults have been inferred to project beneath young depocentres. Moreover, as will later be discussed in more detail, some of the faults shown are notional constructs to provide boundaries between rock units in areas of limited exposure. As a result, to keep this study focused and of manageable length, it will concentrate on faults that show clear relationships to Late Cenozoic extension, and subsequent maps will be simplified to emphasize this evidence. Older faults, or faults that have been inferred as structural constructs, will be discussed only where relevant to this history of young extension.

The Blagoevgrad Basin and surroundings

The Blagoevgrad Basin is a *c.* 40 km by 10 km terrestrial depocentre bounding the western and northern margins of the Rila Massif between Blagoevgrad and Sapareva Banya (Fig. 3). Exposure is very limited except in the badland landscape of the 'Stobski Piramidi' (in the footwall of the Rila Fault; Fig. 3; see below) and in occasional roadcuts. The local stratigraphy, after Zagorchev (1992*a*, 2001*a*), begins with a basal red polygenetic conglomerate, overlain by polygenetic conglomerate interbedded with sand and clay, the Pokrovnik Formation. This is followed by, or interbedded with, stacked white, yellow and green fluvial sand and clay, interbedded with gravel lenses, of the Dzherman Formation. Sites in this formation at Kocherinovo and Mursalevo have yielded characteristic Turolian mammals, including the giraffe *Helladotherium* sp., the hipparion *Cremohipparion mediterraneum*, the hyaena *Adcrocuta eximia*, the gazelle *Gazella brevicornis*, and the suid *Microstonyx major* (Nikolov 1985). In modern nomenclature (see Westaway *et al.* 2004, fig. 6), these species coexisted during biozones MN11 (*c.* 9.0–8.2 Ma) and MN12 (*c.* 8.2–7.1 Ma), in the Meiotian stage of the Late Miocene. This unit is followed unconformably by stacked cross-bedded white and yellow fluvial gravels and sands, of the Barakovo Formation, of inferred (?)Pontian to Late Pliocene (Romanian) age. Finally, at the western margin of the Rila Massif, the eroded top of the Barakovo Formation is covered by slope wash, of inferred Eopleistocene (i.e. Early Pleistocene) to Pleistocene (i.e. Mid–Late Pleistocene) age, known as the Badino Formation.

The Saparevo normal fault

Arguably the clearest indication of active extension in this region is provided by the NW-dipping

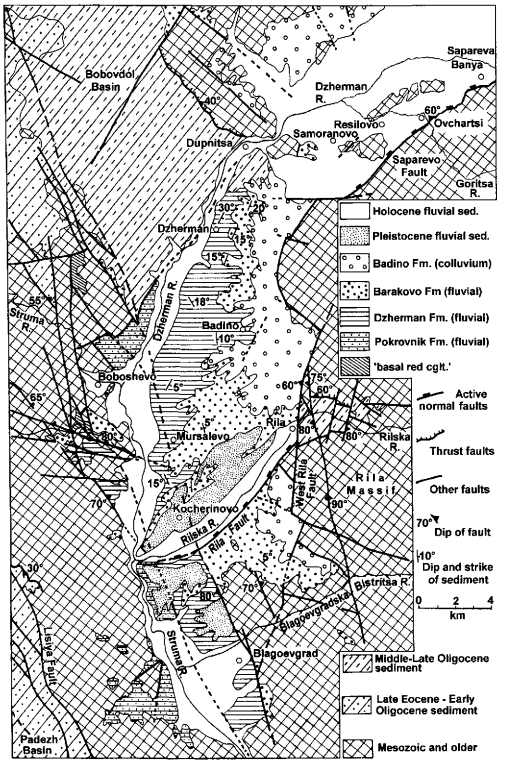

Fig. 3. Map of the Blagoevgrad Basin, adapted from Zagorchev (1992*a*, fig. 9), with additional information from Shipkova & Ivanov (2000, fig. 1) and my own field observations. Dupnitsa was known as Stanke Dimitrov in the communist era and is still labelled as such on some modern maps. Estimated ages of the Late Cenozoic formations defined within this basin are discussed in the text. The Kalin pluton forms the footwall of the Saparevo Fault in the NW part of the Rila Massif. However, it is not individually labelled, as no pre-Cenozoic rocks are differentiated on this map.

Saparevo normal fault near Dupnitsa (Figs 3 and 4a,b), which has uplifted the West Rila horst in its footwall by *c.* 2 km relative to the depositional surface in its hanging wall (*c.* 2600 against *c.* 600 m above sea level (a.s.l.)). The fault plane is well exposed at the base of this footwall escarpment (Fig. 4c), as a smooth, relatively fresh-looking rock surface, locally in granite of the Kalin pluton, which intrudes Late Precambrian basement (see Zagorchev 2001*a*). This is one of many geochemically similar plutons, designated as the 'South Bulgarian granitoids' (see Zagorchev 1998*a*). Although the Kalin pluton is not dated, others in this grouping have been Rb–Sr dated to the Hercynian orogeny

(a)

(b)

(c)

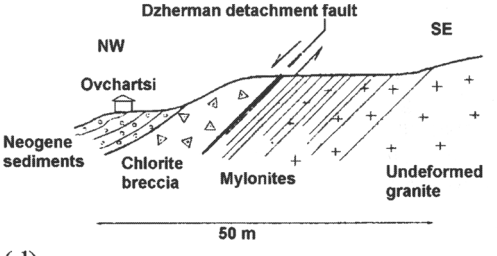

(d)

Fig. 4. The Saparevo normal fault between Dupnitsa and Sapareva Banya. (**a**) View looking east obliquely towards this fault from [FM 77398 81787], *c.* 1 km east of Samoranovo, with Resilovo in foreground. View shows characteristic footwall morphology of a steep planar normal fault. Viewpoint is *c.* 600 m a.s.l.; summit skyline in footwall is *c.* 2600 m a.s.l.. (**b**) View looking S20°E at the footwall escarpment from [FM 81655 82272], between Resilovo and Ovchartsi, showing characteristic 'flat-iron' facets being incised by small streams to form 'wineglass canyons'. (**c**) Close-up view of the base of the footwall escarpment at Ovchartsi, at [FM 83571 82236], showing a relatively fresh smooth rock surface (in Late Palaeozoic granite) degrading upwards into a more eroded rock face and buried downslope by a pediment of slope scree. This site is located just east of the point where the Goritsa River crosses the Saparevo Fault in Figure 3. (**d**) Interpretation of the locality illustrated in (**c**), from Shipkova & Ivanov (2000, fig. 3). The interpreted 'chlorite breccia' corresponds to the slope talus depicted in (**c**), and the interpreted 'mylonite' corresponds to the brittle joint set oriented subparallel to the fault plane in (**c**). Universal Transverse Mercator (UTM) position fixes such as [FM 77398 81787], indicating the co-ordinates of sites to the nearest metre, were obtained in the field using a handheld GPS receiver. The letters indicate the 100 km × 100 km UTM quadrangle; the five-digit numbers indicate distance east and north, respectively, from the SW corner of this quadrangle. (See text for discussion.)

(*c.* 340–240 Ma; Zagorchev & Moorbath 1986; Zagorchev *et al.* 1989*a*). The geochemically similar Kavala (Symvolon) granite in northern Greece, also assigned to this grouping (see Zagorchev 1998*a*), has also yielded U–Pb dates on zircons of *c.* 335 Ma (Kokkinakis 1980; Dinter *et al.* 1995; see also below). The Kalin granite has experienced pervasive brittle deformation leading to the formation of a fracture set oriented subparallel to the escarpment face, plus other sets at different orientations (some visible in Fig. 4c), which contribute to producing the irregular appearance of this fault escarpment. In places, the fault surface is preserved only as small facets, with dimensions of tens of centimetres, bounded by the intersection lineations between these fracture sets. This fault surface is not precisely planar: measured up a *c.* 5 m face its orientation varied upward from dip 60° towards N53°W to dip 40° towards N60°W. However, it seems clear that the escarpment rising *c.* 2 km above this faceted fault surface represents the uplifted footwall of this fault, its degree of weathering increasing upslope. No striations were found that could indicate the precise extension sense. However, the heave on this normal fault (between its footwall and hanging-wall cutoffs) indicates several kilometres of extension.

Shipkova & Ivanov (1999, 2000, 2001) have proposed a radically different interpretation of this structure, which they call the 'Dzherman detachment'. In their view (Fig. 4d), the Kalin pluton was intruded during Late Cenozoic extension, and became mylonitized at mid-crustal depths before passing upward into the brittle regime and receiving what they interpreted as a 'cataclastic overprint' oriented subparallel to the fault plane. They interpreted what seemed to me to be slope scree in the hanging wall (Fig. 4c) as 'chloritic breccia' (Fig. 4d), its thickness providing an indication to them of the magnitude of the slip on this fault while in the brittle regime. Although no dipping Neogene sediments were visible to me in the Holocene alluvial plain adjoining this normal fault, they concluded that these sediments dip subparallel to the fault plane, thus suggesting that it formed at a low-angle dip, and must thus have accommodated many tens of kilometres of extension in order to exhume material that was initially at mid-crustal depths. This interpretation seems unlikely but is impossible to test in detail because necessary information (e.g. thin sections indicating mylonitization, exposures of Neogene sediment, dates indicating a Neogene intrusion age) are lacking. I return in the Discussion section to the wider question of granite intrusion ages in this region.

The Kyustendil normal fault

West of Kyustendil, beyond the western margin of the Blagoevgrad Basin (Fig. 2), the northern margin of the Osogovo mountains is abruptly truncated by a planar escarpment, dropping from *c.* 1800 m to *c.* 900 m a.s.l.. This feature continues in line with S75°W strike for *c.* 20 km to the border with Macedonia at Gyushevo (Fig. 2), then for *c.* 30 km farther inside Macedonia. It has been mapped (Fig. 2) as the footwall escarpment of a significant active normal fault (see Zagorchev 1992*a*).

Kyustendil town occupies the SW corner of the Kyustendil Basin, another (?)Mid-Miocene to (?)Early Pliocene terrestrial depocentre now *c.* 500 m a.s.l. (see Vatsev & Bonev 1994, or Zagorchev 2001*a*, for details of its stratigraphy). The Struma enters this basin at the outlet of the Zemen gorge at Razhdavitsa, then flows across this basin for *c.* 15 km to Nevestino, where it enters the Skrino gorge that leads to the Blagoevgrad Basin at Boboshevo (Figs 2 and 3). There is abundant evidence throughout this area, including within the Skrino gorge (notably at Pastuh [FM 57452 74256]), of a staircase of Struma terraces, indicating significant young fluvial incision.

The southern margin of the Kyustendil Basin was inspected for evidence of normal faulting for *c.* 15 km distance between Kyustendil and Nevestino (at [FM 51991 79937]). The abrupt footwall escarpment of the Kyustendil normal fault seems to follow the margin of this basin for a few kilometres directly south of Kyustendil town. However, farther east it appears to die out, as the basin margin becomes much more subdued. The suggestion in Figure 2 that it continues ENE beneath this basin seems conjectural, as no supporting evidence (such as warped or offset river terraces) could be observed.

The Rila normal fault

Unlike farther NE, the contact between basement and Neogene sediments at the western margin of the Rila Massif between Dupnitsa and Rila town (Fig. 3) shows no clear geomorphological evidence of active normal faulting. However, a clear active normal fault zone, which I call the Rila Fault, strikes SW, oblique to the margin of this massif (Figs 3 and 5a). This fault is clearest just west of Rila town (Fig. 6a), where its *c.* 300 m high footwall escarpment is formed in basement (Fig. 5a and b). Farther SW (Fig. 6b), the fault cuts through the Neogene sequence of the Blagoevgrad Basin, creating the 'Stobski Piramidi' badland landscape in deposits of the

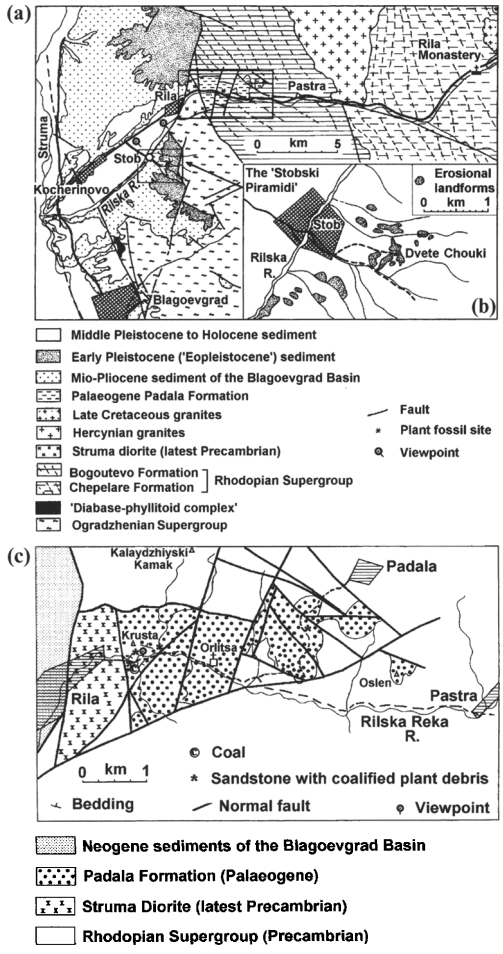

Fig. 5. (**a**) Map of the SE Blagoevgrad Basin, showing the locations of the Rilska river gorge and the Rila normal fault. (**b**) Inset showing the dissected landscape of the Stobski Piramidi nature reserve in the footwall of the Rila normal fault. (See (**a**) for location.) (**c**) Map of the lower part of the Rilska gorge through the Palaeogene Padala Formation. (See (**a**) for location.) Adapted from Zagorchev (1995, fig. 40) and Zagorchev *et al.* (1999, fig. 3). (See text for discussion.)

Barakovo and Badino formations in its footwall (Fig. 5a and c). In contrast, its hanging wall, drained axially by the Rilska River, is covered by inset Pleistocene or Holocene sediments (Figs 3 and 5a). The height of this footwall escarpment decreases gradually southwestward from Stob, becoming minimal by its intersection with the Struma River (Fig. 3).

An approximate in-line continuation of this fault zone ENE of Rila town can be traced to the vicinity of Padala (Fig. 5c), and may be responsible for the local downthrow of conglomerates of the Palaeogene Padala Formation (see Zagorchev *et al.* 1999; see also below) relative to the basement farther south, which has facilitated preservation of these sediments.

The Rilska gorge section

The stratigraphic section exposed in the gorge of the Rilska River (Fig. 6c) has recently been the subject of controversy regarding possible reinterpretation of it as evidence of Late Cenozoic low-angle normal faulting (see Shipkova & Ivanov 1999, 2000, 2001). As already noted, the local outcrop has been regarded as a pocket of Palaeogene conglomerate, which overlies metamorphic basement and has been fortuitously preserved as a result of young normal faulting that has downthrown it relative to the adjoining basement (see Zagorchev *et al.* 1999). Coal beds and other fragments of plant remains have long been reported in this deposit (e.g. Bonchev 1912; Konyarov 1932; Moskovski 1983; Marinova 1991; Zagorchev 1998*a*; Zagorchev *et al.* 1999), suggesting a sedimentary origin, presumably marsh at the foot of a hillslope at the margin of the basement upland. Shipkova & Ivanov (1999, 2000) have proposed, on the contrary, that this conglomerate is a fault breccia and the adjacent basement surface is mylonitized (Fig. 6d), the contact between the two thus indicating a low-angle normal fault surface with a *c.* 20° dip, along which the basement to the east has uplifted from mid-crustal depths during large-scale Late Cenozoic extension. However, Shipkova & Ivanov (1999, 2000) offered no explanation for the plant material found in this sediment, and their interpretation that it is a cataclasite was based on sedimentary characteristics (notably, angularity of clasts; fining-upward characteristics; clasts and matrix have same composition, matching the local basement; micas in the matrix show chloritization) that could also be expected in a slope deposit derived from the local basement.

The contact between Padala conglomerate and basement is well exposed as a result of recent widening of the road to Rila monastery, east of Orlitsa monastery at [FM 79016 66340]; it seemed to me to be an unconformity surface, dipping west at *c.* 30°. Moreover, I could see no evidence of mylonitization of the underlying basement, whose upper surface appeared weathered, not faulted or deformed in a ductile manner. However, this conglomerate is broken up by minor normal faulting, which post-dates its deposition; for instance, one fault at [FM 78953 66350] dips at 72° towards S80°W. I did not observe any clear evidence of plant remains in this conglomerate (several of the sites depicted

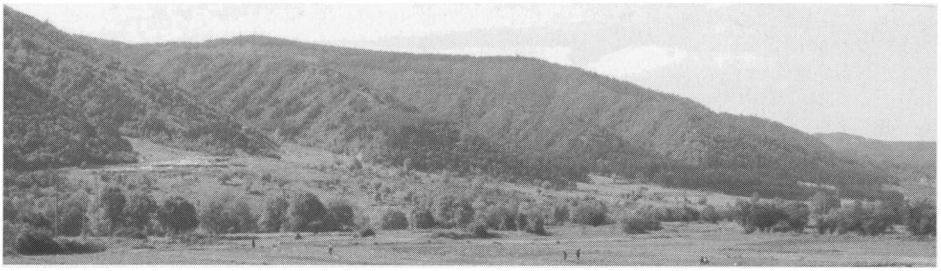

(a)

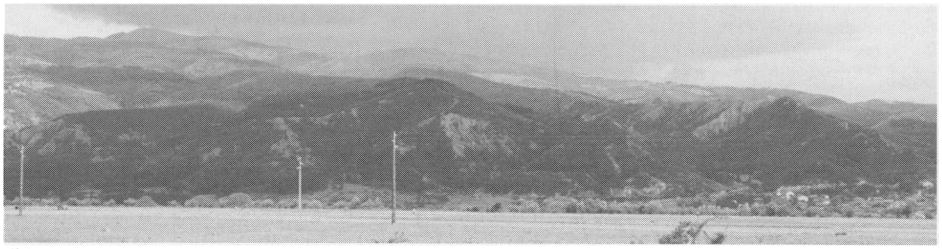

(b)

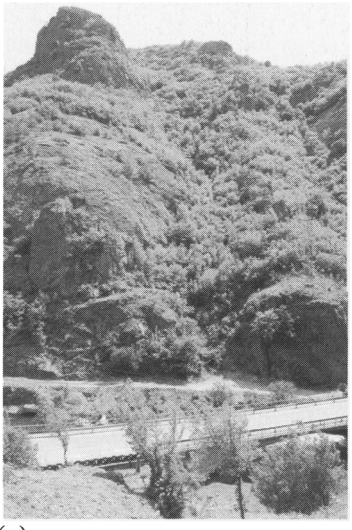

(c)

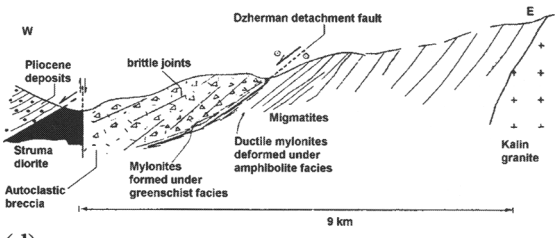

(d)

Fig. 6. (**a**) Oblique view looking SSE from [FM 75370 65032], just SW of Rila town, towards the S35°W-striking Rila normal fault. Alluvial fans prograde from wineglass canyons, through the faceted range front; the downthrow from the tops of the facets shown to the foreground hanging-wall alluvial plain, at *c.* 500 m a.s.l., is *c.* 300 m. (**b**) View looking ESE at the Rila normal fault from [FM 73198 63489], on the road between Rila town and Stob (the village in the right middle distance), *c.* 3 km SW of the viewpoint in (**a**). The footwall escarpment is now only *c.* 100 m high, compared with *c.* 300 m; its height continues to decrease to the SW, dying out completely *c.* 5 km farther SW. Erosion of the Neogene sediment that has been uplifted in this footwall has created the erosional landscape known as the 'Stobski Piramidi' (Fig. 5b). The summit in the left background, at 2386 m a.s.l., is *c.* 15 km away, in the interior of the Rila Massif. The bulk of the local relief shown is thus unrelated to the small amount of throw indicated by the height of the footwall escarpment along the range front. (**c**) View looking south, from [FM 77958 66740], across the Rilska river gorge between Rila town and Orlitsa, showing Palaeogene conglomerate of the Padala Formation dipping at *c.* 10° towards S56°E on the south flank of the gorge. (**d**) Interpretation of the section along the Rilska gorge through the locality illustrated in (**c**), from Shipkova & Ivanov (2000, fig. 2). The interpreted 'autoclastic breccia' corresponds to the conglomerate depicted in (**c**). (See text for discussion.)

in Fig. 6c are now inaccessible because road-widening has converted the gorge flanks into vertical cliffs), but the literature reports (dating back to the early 19th century) of coal, plant leaves and stems, and pollen indicating an Oligocene age (summarized by Zagorchev *et al.* 1999) seem clear enough.

Other inferred low-angle normal faulting

West of the Blagoevgrad Basin is an elongated (*c.* 10 km by 3 km) S20°E-trending outcrop of Palaeogene sediment, the Padezh Basin (Figs 2 and 3). Now situated *c.* 600 m a.s.l., this is dated to the Priabonian to Early Oligocene, and records a transition from terrestrial to marine conditions (Zagorchev *et al.* 1989*b*; Zagorchev 2001*a*). These only partly lithified sediments, which attain a thickness of many hundreds of metres, are strongly tilted ENE and broken up by post-depositional faulting; they are exposed along the roads from Blagoevgrad to Padezh and the nearby villages of Leshko and Gabrovo; for instance, marine limestone (Padezh Formation) dipping at 50° towards N65°E at [FM 64951 42801] and the underlying fluvial sand, conglomerate and lacustrine claystone (Logodazh Formation) dipping at 55° towards N74°E at [FM 62288 44446]. This marine basin is thought to have been linked to the open sea to the NW, and is the farthest south where marine sediments from this time are documented (see Zagorchev 1992*a*). This Palaeogene sequence thickens westward across this basin, suggesting that the clastic input was from the Vlahina mountain range to the west (Fig. 2). These sediments are locally capped by up to *c.* 50 m of stacked fluvial sand and gravel assigned to the Barakovo Formation (see above), which has also been derived from Vlahina. The literature is unspecific as to the tectonic setting during deposition in this basin. There is of course no requirement for any contemporaneous crustal deformation (independent of rock uplift caused erosion, and subsidence caused by deposition); these sediments could simply have accumulated in a sag basin adjacent to the eroding Vlahina mountains. Their subsequent deformation has been attributed (e.g. by Zagorchev 1992*a*) to a combination of thrusting and NNW–SSE-directed right-lateral strike-slip in the Early–Mid-Miocene, between the end of local deposition and the start of crustal extension.

Burchfiel *et al.* (2000, 2003) suggested, on the contrary, that these sediments were deposited during Eocene to Oligocene extension, and attributed their strong eastward tilting to downthrow to the west on a major normal fault system, which they inferred to be associated with extension across the Blagoevgrad Basin and to have tilted to a low-angle dip to achieve the steep dip of the sequence in the Padezh Basin. I return to these views, which seem conjectural, in the Discussion section.

The Simitli Basin

South of Blagoevgrad (Fig. 7), the Struma flows for *c.* 10 km, in a gorge through basement, to the Simitli Basin. This *c.* 20 km by 5 km basin is in the hanging wall of the Krupnik normal fault to the SSE (Fig. 8). On leaving it, the Struma flows into this footwall, then along the Kresna gorge for *c.* 15 km to the Sandanski Basin.

Kotzev *et al.* (2001) suggested that the Krupnik Fault is left-lateral, but this view seems to have no basis. The detailed literature on it (e.g. Botev *et al.* 2001; Meyer *et al.* 2002) makes clear that it is an active normal fault, as seems obvious from the local structure and geomorphology (Fig. 8). It was indeed the probable source of the 4 April 1904 Krupnik earthquake (e.g. Zagorchev 1992*a*, 1995; Meyer *et al.* 2002; see Ambraseys 2001), the largest event known in the Balkan region (magnitude *c.* 7.8).

The stratigraphy of this basin (see Marinova & Zagorchev 1990; Zagorchev 2001*a*) begins with a coal-bearing unit, the Oranovo Formation, dated to the Sarmatian from pollen. This is overlain in the stratigraphic scheme used by Meyer *et al.* (2002) by a stacked sequence of inferred Meiotian age, comprising the Chernichevo, Gradevo and Simitli Formations: the first two consisting of conglomerate and the last of fluvial and lacustrine sandstone and siltstone with conglomerate interbeds. In contrast, rather than describing a layer-cake sequence, in the Zagorchev (2001*a*) scheme these deposits are interpreted as marking a lateral facies variation: the coarser Chernichevo Formation at the northern and western margins of the basin with the finer deposits in more distal areas. These deposits have been dated to the Meiotian using pollen (Zagorchev 2001*a*). They are overlain by stacked fluvial sand and conglomerate that is assigned to the Kalimantsi Formation (defined within the Sandanski Basin farther south; see below). Outliers of this deposit crop out on the crest of the Krupnik Fault footwall (Fig. 8a and b), suggesting that when deposited it was continuous between the Simitli and Sandanski basins.

Near Brezhani, this uppermost member of the Kalimantsi Formation has yielded fossil evidence of the bovid *Gazella* (*Tragoportax*) aff. *gaudryi* (Nikolov 1985). Assuming correct species identification, this is a Turolian (latest Miocene) taxon that spanned biozones MN11–12 (the Meiotian)

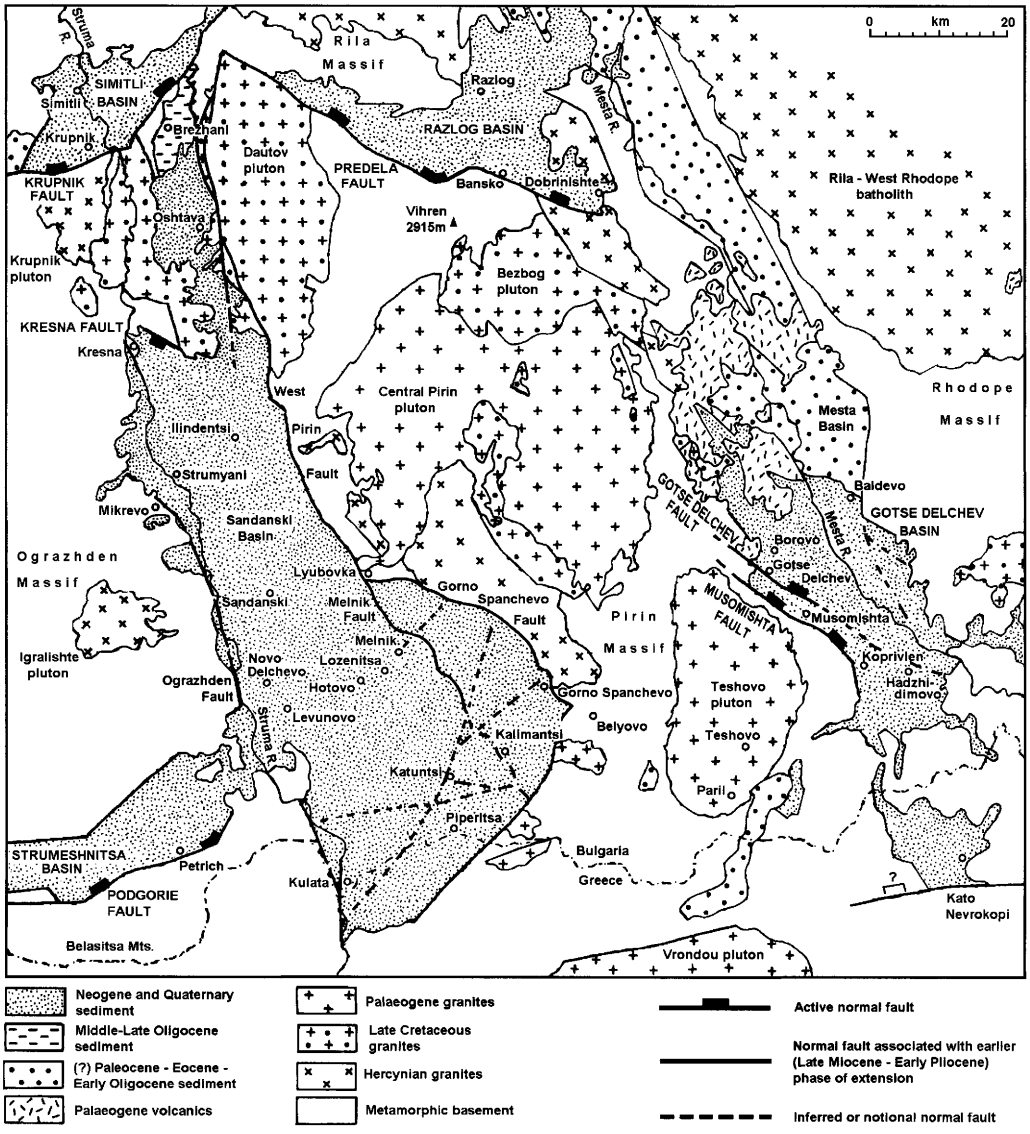

Fig. 7. Map of the southern part of the study region, showing the Simitli, Razlog, Sandanski and Gotse Delchev basins, simplified from Zagorchev (1995, fig. 2). The distinction between Hercynian, Late Cretaceous and Palaeogene granites should be noted; this is supported by dating (e.g. Zagorchev & Moorbath 1986; Zagorchev *et al.* 1989*a*) and geochemical and isotopic analysis (e.g. Zagorchev 1995). Faults older than the Late Cenozoic are not shown, except for the reverse fault along the eastern margin of the Palaeogene Brezhani Basin, which is labelled with ticks on its uplifted hanging wall.

and MN13 (the Pontian) (see Gentry & Heizmann 1996). However, in the northernmost Sandanski Basin farther south, near Kresna, the uppermost member of the Kalimantsi Formation has yielded fossil evidence of the mastodon *Anancus arvernensis* (Nikolov 1985), a Pliocene species (see Athanassiou & Kostopoulos 2001). From the evidence in this area this sedimentary unit is thus not reliably dated and may be diachronous.

The Brezhani Basin comprises a *c.* 2 km by 8 km pocket of Late Oligocene terrestrial sediment also in the footwall of the Krupnik Fault, between the Simitli and Sandanski basins (Figs 7

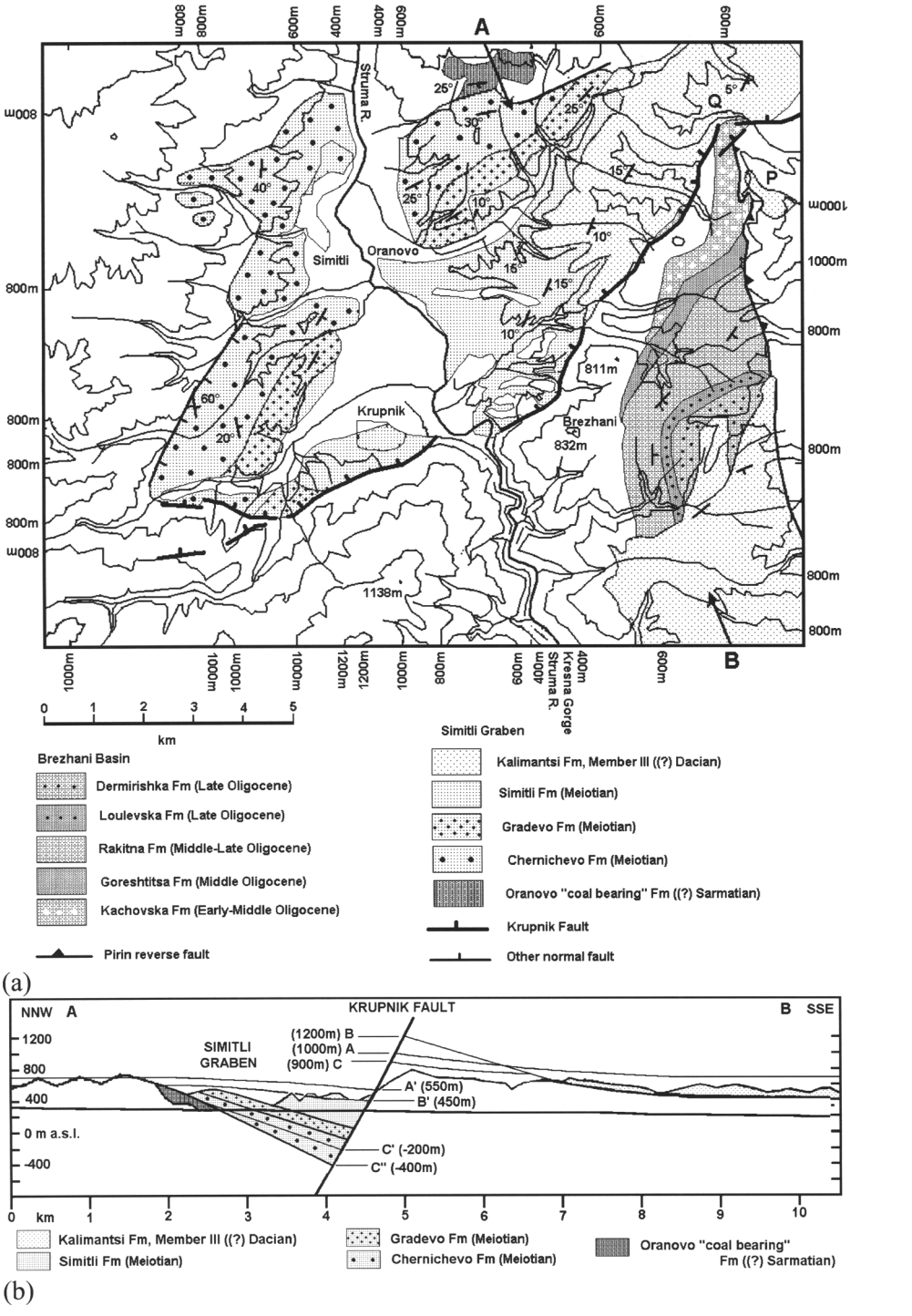

Fig. 8. (**a**) Map of the Simitli Basin. (**b**) Cross-section through the Krupnik Fault. Adapted from Meyer *et al.* (2002, fig. 3), with additional information from Marinova & Zagorchev (1990). Points A, A′, etc. are labelled to facilitate the discussion in the text of amounts of vertical slip on the Krupnik Fault and amounts of erosion from its footwall.

and 8a). Its succession consists of five formations: two (the Goreshtitsa and Loulevska) contain lignite, the others being siltstone, sandstone and conglomerate (see Marinova & Zagorchev 1990; Zagorchev 2001*a*). After deposition, this basin was partly buried by (?)Early Miocene overthrusting from the east (see Zagorchev 1995); in the south it was later unconformably overlain by the Kalimantsi Formation (Figs 8 and 9).

Previous studies (e.g. Meyer *et al.* 2002) have inferred that the whole Simitli Basin succession

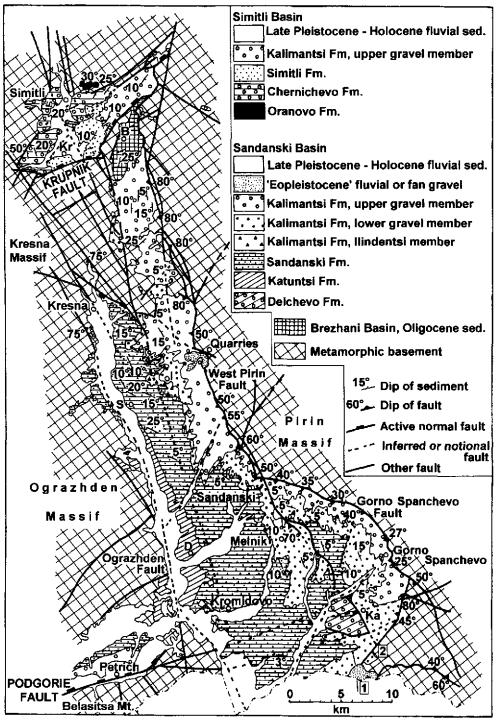

Fig. 9. Map of the Sandanski Basin, also summarizing detail for the Simitli Basin, adapted from Zagorchev (1992*a*, fig. 8). B, Brezhani; D, Novo Delchevo; I, Ilindentsi; Ka, Kalimantsi; Kr, Krupnik; S, Strumyani. 1 and 2, alternative positions for the southern end of the Melnik Fault, from Kojumdgieva *et al.* (1982) and Zagorchev (1992*a*). It should be noted that, as drawn here, by appearing to juxtapose older sediment to the west against younger sediment to the east, this southern end of the Melnik Fault appears to show downthrow to the east, not the downthrow to the west illustrated in Fig. 10b, ii. As noted in the text, there is ambiguity here regarding the precise position of this fault and also regarding the correlation of the sediment west of it (illustrated here as the Delchevo Formation): whether it correlates laterally with the Katuntsi Formation, and is thus older than the Sandanski Formation, or not.

accumulated during extension, in the hanging wall of the Krupnik Fault, thus placing the start of extension in the Sarmatian (*c.* 13 Ma). Meyer *et al.* (2002) thus estimated a time-averaged vertical slip rate of *c.* 0.1 mm a^{-1} and a total of *c.* 1.3 km of vertical slip (C–C″ in Fig. 8b), whereas Zagorchev (1992*a*) estimated *c.* 0.25 mm a^{-1} and *c.* 3.5 km instead. In the east (P–Q in Fig. 8a), Meyer *et al.* (2002) estimated the offset of the base of the Kalimantsi Formation as *c.* 600 m (from *c.* 450 to *c.* 1050 m a.s.l.), implying a vertical slip rate of *c.* 0.1 mm a^{-1} if its age is 6 Ma (or *c.* 0.09 mm a^{-1} if 7 Ma), suggesting that the slip has been uniform at this rate. However, the greater altitude of the basement in the footwall farther west (> 1100 m, west of the Kresna gorge; Fig. 8b) suggests that this part of the Krupnik Fault has slipped faster.

Given that deposition of the Kalimantsi Formation straddled the eastern part of the Krupnik Fault that appears to have slipped least, all the earlier formations may have also been deposited across this fault farther west, but have since been removed from its footwall by erosion. If so, and all its slip is further assumed to post-date the Kalimantsi Formation, then an estimated thickness of 950 m (A′–C″ in Fig 8b) could have been eroded from the footwall, in which case the vertical slip on the western Krupnik Fault could have been as much as C″–B (*c.* 1600 m) plus A′–C″, or *c.* 2550 m. Furthermore, if all this slip occurred after deposition of the Kalimantsi Formation (since a nominal time of *c.* 3 Ma; see further discussion below) then the vertical slip rate could be as high as *c.* 2550 m in *c.* 3 Ma or *c.* 0.85 mm a^{-1}. If so, then the *c.* 250 m of incision by the Struma river from *c.* 550 m (A′ in Fig. 8b) to its present level of *c.* 300 m a.s.l. occurred at a time-averaged rate of *c.* 0.08 mm a^{-1}, with a time-averaged incision rate of *c.* 0.62 mm a^{-1} at the footwall cutoff (for *c.* 1850 m of incision since 3 Ma).

Conversely, if one takes the estimate of *c.* 0.1 mm a^{-1} from Meyer *et al.* (2002) as a lower bound to the vertical slip rate on the Krupnik Fault, then the *c.* 0.08 mm a^{-1} time-averaged rate of incision by the Struma in the hanging wall requires an incision rate of *c.* 0.18 mm a^{-1} in the footwall cutoff, requiring *c.* 540 m of incision since *c.* 3 Ma, placing the contemporaneous land surface at the footwall cutoff at *c.* 840 m a.s.l.. This is significantly higher than the modern flanks of the Kresna gorge, which only reach to *c.* 600 m a.s.l., indicating that the present morphology of this gorge significantly underestimates the amount of incision that has occurred. Presumably, when this gorge began to develop the Struma cut into the lowest point in the former

depositional surface of the Kalimantsi Formation, causing it to become localized in its present position, where it subsequently incised through the base of the Kalimantsi Formation into the underlying metamorphic basement; it is thus an example of superimposed drainage.

The Sandanski Basin

The Late Cenozoic sequence in the Sandanski Basin (Figs 7 and 9), with total thickness >1600 m, begins with the Delchevo Formation, of Badenian to Sarmatian or Meiotian age, consisting of red to green silty fluvial sandstone with siltstone, shale, clay and fine conglomerate, plus occasional tuff and limestone beds (e.g. Kojumdgieva *et al.* 1982; Zagorchev 1992*a*). It has yielded, at Levunovo, teeth of the antelope *Micromeryx flourensianus* (e.g. Kojumdgieva *et al.* 1982; Nikolov 1985), an Astaracian (late Mid-Miocene; biozones MN6–8) taxon (see Kojumdgieva *et al.* 1982; Gentry & Heizmann 1996) and, at Novo Delchevo, a tooth of the Vallesian elephant *Choerolophodon serridentinoides* (e.g. Kojumdgieva *et al.* 1982; Nikolov 1985). Similar sediments in the adjacent Serrai Basin in northern Greece (Fig. 1a) are late Vallesian (biozone MN10) from their mammal faunas (e.g. Karistineos & Georgiades-Dikeoulia 1986). The Katuntsi Formation, consisting of red conglomerate, has been designated (e.g. Zagorchev & Dinkova 1990) near the eastern margin of the Sandanski Basin (Fig. 9) and interpreted as a proximal facies that interfingers with the more distal Delchevo Formation (Zagorchev 1992*a*), but is not directly dated.

The Sandanski Formation, of reported Meiotian age (e.g. Zagorchev 1992*a*), consists of coarser fluvial sandstone, sometimes cross-bedded, with silty interbeds. The Kalimantsi Formation, of reported Pontian to (?)Romanian or (?)Dacian age (e.g. Zagorchev 1992*a*), consists mainly of conglomerate, typically formed of rounded clasts of granite from the Palaeogene Central Pirin pluton to the east (Fig. 7). However, its lowest member, the Ilindentsi Member, comprises carbonate-cemented clasts of the (?)Precambrian Dobrostan Marble. It is found on the eastern flank of the Sandanski Basin, adjacent to outcrop of this marble in the western Pirin Massif (Figs 9 and 10a), the clast size ranging up to huge olistostromes with dimensions of many tens of metres.

The above sediments typically dip east at *c.* 5–20° (Figs 9 and 10b), indicating significant downthrow since their deposition on normal faults bounding the eastern basin margin (see Zagorchev 1992*a*). North of Lyubovka, this margin is bounded by the S25°E-striking West Pirin normal fault (Figs 9 and 10a). At Lyubovka, this fault is considered to splay, with one strand (the Melnik Fault) continuing S25°E into the basin interior, and the other (the Gorno Spanchevo Fault) (Fig. 10c and d) branching eastward then bending progressively to the right as it follows the basin margin, reaching *c.* 6 km from the Melnik Fault before rejoining it near the border with Greece (Fig. 9).

In this southern part of the basin, the lower part of the Sandanski Formation contains the Kromidovo mammal site (Fig. 9), with a diverse Turolian or 'Pikermian' fauna (see, e.g. Kojumdgieva *et al.* 1982, or Nikolov 1985, for species lists). Species include the hipparions *Cremohipparion mediterraneum* and *C. matthewi*, indicative of biozones MN11–13 (*c.* 9.0–5.4 Ma) and MN12–13 (*c.* 8.2–5.4 Ma), respectively (e.g. Bernor *et al.* 1996), and the primate *Mesopithecus pentelici*, also from MN12–13 (e.g. Andrews *et al.* 1996). From its stratigraphic position, this site is assigned to biozone MN12 (*c.* 8.2–7.1 Ma) (e.g. Kojumdgieva *et al.* 1982). The upper part of the Sandanski Formation has yielded fish fossils indicative of brackish conditions (e.g. Kojumdgieva *et al.* 1982; Palmarev 1982), suggesting a correlation with the latest Meiotian marine transgression that reached as far north as the Serrai Basin (e.g. Gramman & Kockel 1969; Karistineos & Georgiades-Dikeoulia 1986). Higher up the sequence, near Melnik (Figs 9 and 10b, i), the Kalimantsi Formation has yielded the Pliocene mastodon *Anancus arvernensis* (e.g. Kojumdgieva *et al.* 1982; Nikolov 1985), indicating a significantly younger age.

In the extreme south of this basin the stratigraphy becomes more problematic. Kojumdgieva *et al.* (1982) designated the Kalimantsi Formation stratotype along the road from Kalimantsi to Belyovo, in the Melnik Fault footwall and the Gorno Spanchevo Fault hanging wall (Fig. 10b, ii). This sequence passes upward from fluvial sands, similar to the Sandanski Formation elsewhere in the basin, to conglomerates, with four mammal sites (Kalimantsi 1–4; Fig. 10b, ii). Site Kalimantsi-3 has yielded *Cremohipparion matthewi*, again suggesting biozone MN12. However, Kalimantsi-1, with several characteristic Vallesian species (see, e.g. Kojumdgieva *et al.* 1982, or Nikolov 1985, for lists) including the rhinoceros *Aceratherium zernowi* (from MN9–10 according to Heissig 1996; see also Geraads *et al.* 2001), is considered significantly older.

Kojumdgieva *et al.* (1982) deduced from the biostratigraphic ages that the sediments designated as the Sandanski and Kalimantsi Formations overlap, but Zagorchev (1992*a*) disputed this. The biostratigraphic evidence suggests that

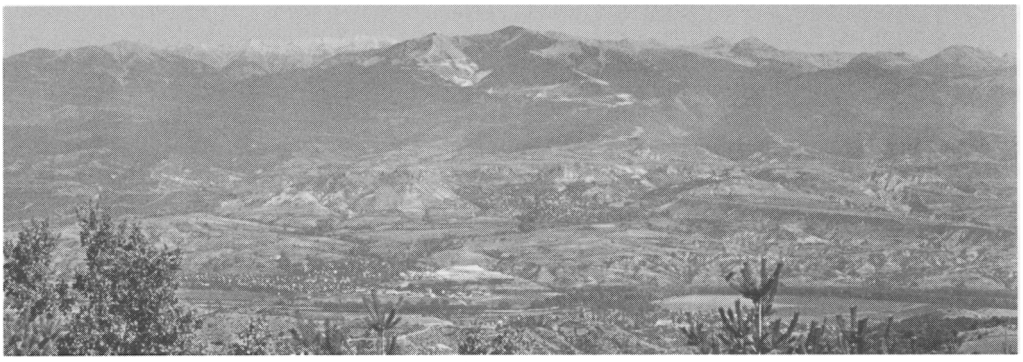

(a)

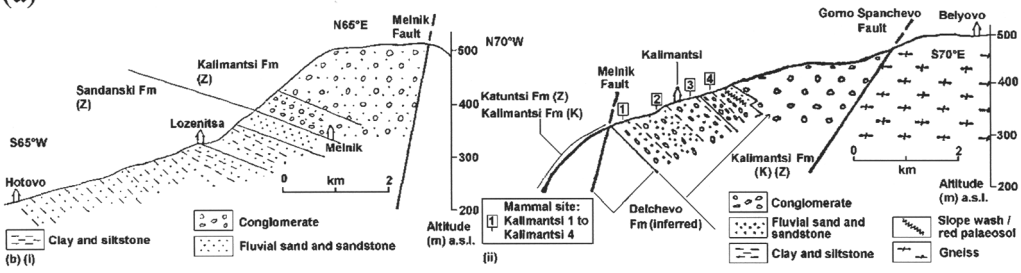

(c)

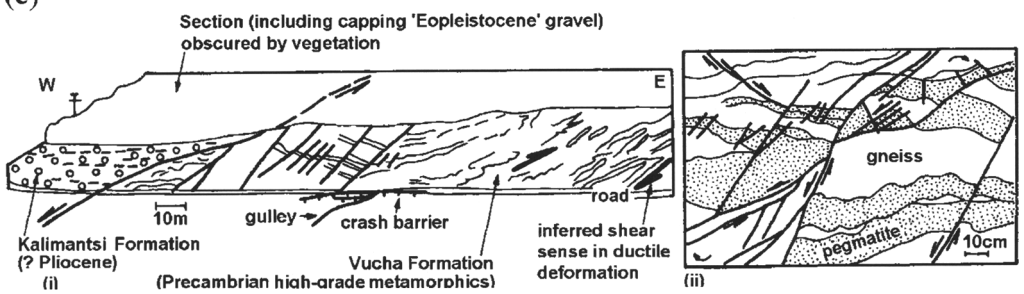

(d)

they do overlap in the extreme south of this basin, making it unfortunate that this is where the latter formation has been defined. As it would now appear that much of its stratotype lies within the age span of the Sandanski Formation, redefinition seems essential. However, the uppermost Kalimantsi Formation (which is important to the present study for dating the end of extension and/or the start of regional uplift across this basin) seems to have been defined in an unambiguous manner, permitting correlation of it throughout the basin.

The West Pirin Fault

At Ilindentsi (Figs 7 and 10), outcrop of the Ilindentsi member is observed (e.g. from [FM 86418 13202]) to be back-tilted east at *c.* 10°. A traverse is possible from here, at *c.* 400 m a.s.l., up the footwall escarpment of the West Pirin Fault to the source area of its clasts of Dobrostan Marble in a quarry at [FM 91449 16729], at *c.* 1100 m a.s.l. This *c.* 6 km traverse passes upward through fluvial deposits of the Kalimantsi Formation, with clasts predominantly of marble lower down and of Palaeogene granite higher up. Locally, fluvial units are observed to be separated by palaeosols; and their sequence is capped by gravel of inferred 'Eopleistocene' age that has not been offset by normal faulting (see Zagorchev 1992*a*). This pervasive cover of sediment makes the precise location of the footwall cutoff difficult to establish, and there is locally no geomorphological evidence of active slip on the West Pirin Fault. Zagorchev (1992*a*) estimated the total vertical slip on this fault as *c.* 3500 m, of which *c.* 100 m was considered to post-date the Kalimantsi Formation. However, it is unclear how this *c.* 100 m post-depositional offset was established, as these sediments are reportedly present only in the hanging wall of the fault.

Between Ilindentsi and the Struma, the Sandanski Formation typically dips east at *c.* 10–15° (e.g. Zagorchev & Dinkova 1990; Zagorchev 1992*a*, 1995; Fig. 9). As shown in Figure 10a, its eroded surface is terraced at many different levels, designated as pediments or river terraces (see Zagorchev 1992*a*, 1995). No evidence could be observed of any faulted offsets of these levels. Near Ilindentsi, the footwall cutoff of the West Pirin Fault is observed *c.* 900 m a.s.l. Zagorchev (1992*a*, 1995) estimated by projection that the base of the sequence in the Sandanski Basin beside it is *c.* 1000 m below sea level; he correlated this palaeo-land surface with an erosion surface now *c.* 2500 m a.s.l. in the Pirin Massif. As a result, he partitioned the vertical slip on this fault with *c.* 1900 m of hanging-wall subsidence (below the present footwall cutoff) and *c.* 1600 m of footwall uplift. However, this estimate is clearly an upper bound to the total slip, as the correlation of erosion surfaces (see Zagorchev 1992*a*) seems intuitive and difficult to test.

This fault was also examined farther south at Lyubovka (Fig. 7), around [FM 97208 05650]. It is locally mapped (Zagorchev & Dinkova 1990) as a *c.* 500 m wide fault zone separating the uppermost member of the Kalimantsi Formation from Palaeogene granite of the Central Pirin Pluton, with a local WSW dip of 40–50° (Zagorchev 1992*a*, 1995; Fig. 10). There is locally a rather subdued escarpment bounding the granite, against which the sediments dip at *c.* 10°. This granite is highly weathered, suggesting that it has

Fig. 10. (**a**) View ENE across the Sandanski Basin from its western margin at [FM 82536 09606] near Mikrevo. Light patches near the skyline in the centre of the field of view are *in situ* exposures of the Dobrostan Marble in quarries. Light patches lower down the slope are olistostromes of the same marble within the Ilindentsi Member of the Kalimantsi Formation; they surround Ilindentsi village, which is barely visible. Village lower down to left of field of view is Strumjani. A gravel pediment (of inferred 'Eopleistocene' age; Zagorchev 1992*a*) also passes downslope onto the Ilindentsi Member. It is not cut by normal faulting, indicating that this part of the West Pirin Fault is no longer active. Subhorizontal benches visible at a variety of levels below Ilindentsi are presumed to be terraces of the Struma; no evidence was observed that they are separated by fault scarps. This photograph was kindly provided by I. Zagorchev. (**b**) Cross-sections through the southern Sandanski Basin, adapted from Kojumdgieva *et al.* (1982, figs 4 and 5). (i) Hotovo-Melnik; (ii) Kalimantsi-Belyovo (see Fig. 7 for locations). Both sections are along roads; their average orientations are indicated. In (ii) the conglomerate in the hanging wall of the Melnik Fault was assigned to the Kalimantsi Formation by Kojumdgieva *et al.* (1982) (K) and to the Katuntsi Formation in later studies by Zagorchev (Z) (see Fig. 9). (**c**) View northward to the roadcut exposure of the Gorno Spanchevo Fault at [GL 10582 98279]. Subhorizontally bedded conglomerate of the Kalimantsi Formation is juxtaposed, across a surface that dips west at *c.* 25°, against mylonitized and folded gneiss and amphibolite (with pegmatite veins) of the Vucha Formation of the Rhodopian Supergroup. This contact is sealed by subhorizontal gravel of inferred 'Eopleistocene' age, which is not visible in this view. (**d**) Field sketch (i) and interpretation (ii) of the locality in (**b**), adapted from part of Zagorchev (1995, fig. 25). Zagorchev interpreted the gneiss near the contact with the sediments as pervasively deformed by brittle fractures typically dipping to the west. My alternative impression was that fragments of the gneiss were becoming progressively looser nearer the contact, before weathering out into the overlying regolith. However, the section was evidently much less fresh at the time of my visit than when first examined by Zagorchev.

been locally exposed at the Earth's surface for a significant time. This evidence suggests that this fault is not active at present, although it was presumably important at an earlier stage when slip on it caused the observed tilting of the basin sediment.

The Melnik Fault

The Melnik Fault is readily identifiable in the Melnishka river gorge *c.* 1 km NE of Melnik (Fig. 9), marked by a transition from Kalimantsi Formation conglomerate in its hanging wall to Sandanski Formation sandstone in its footwall. The beds on both sides of it locally dip consistently ENE at *c.* 5–10° (see Fig. 10b, i), indicating back-tilting accompanying downthrow to the west. Both footwall and hanging wall are locally highly dissected by badland erosion, producing the 'Melnishki Piramidi' erosional landscape. The absence of clear differential dissection between the footwall and hanging-wall blocks suggests that little or no active slip is occurring on this fault at present.

Although the absence of basement exposure makes it impossible to estimate the total slip on the Melnik Fault, its slip since the end of deposition of the Sandanski Formation can be roughly estimated. Mapping by Zagorchev & Dinkova (1990) indicates that *c.* 2 km east of this fault near Melnik, the top of this formation is at *c.* 500 m a.s.l. and dips away from this fault at *c.* 5°. It thus projects back to *c.* 700 m a.s.l. at the footwall cutoff (500 m + 2000 m × tan(5°)). Its *c.* 300 m a.s.l. altitude at the hanging-wall cutoff (Fig. 10b, i) thus indicates that the throw since this time has been *c.* 400 m.

West of Melnik, the outcrop passes progressively down-section from the Kalimantsi Formation to the Sandanski Formation (Fig. 10b, i) and then the Delchevo Formation, with no evidence of further disruption by normal faulting. Numerous sections through palaeo-channels are evident locally, at up to *c.* 200 m above the Struma, inset into the Sandanski Formation and overlain by slope deposits, for instance at [FL 98268 97924] near Lozenitsa, *c.* 3 km SW of Melnik and *c.* 100 m above the present level of the Struma (*c.* 340 m a.s.l. against *c.* 240 m). These appear to typically trend SSE, subperpendicular to the modern tributary drainages (along which these channel sections are exposed), and evidently record progressive incision by the Struma to its present level.

In the south, the stratigraphic relationships across this fault are not well resolved. Near Kalimantsi, Kojumdgieva *et al.* (1982) mapped it (1 in Fig. 9) with the Kalimantsi Formation in both footwall to the east and hanging wall to the west (Fig. 10b, ii), although as noted above the former sediments may be part of the Sandanski Formation. Zagorchev & Dinkova (1990) and Zagorchev (1992*a*) located this fault several kilometres farther east (2 in Fig. 9) and interpreted it with the Katuntsi Formation to the west. This requires a complex pattern of local vertical crustal motions, which are inferred to have occurred on a mosaic of normal faults across this area, at positions indicated in Figures 7 and 9. It was not possible to resolve this discrepancy during my fieldwork in the area.

The Gorno Spanchevo Fault

As already noted, this fault is interpreted along the eastern margin of the Sandanski Basin south of Lyubovka. I investigated the contact between Kalimantsi Formation and metamorphic basement of the Rhodopian Supergroup at several localites, it being most accessible near Gorno Spanchevo at *c.* 700 m a.s.l. [GL 10582 98579] on the road from Katuntsi to Gotse Delchev (Figs 9 and 10c,d). This basement is mylonitized, but the mylonitic fabric can be seen to not be parallel to the contact and has also been inferred to have a top-to-the-east sense of shear (e.g. Zagorchev 1995), so it could not be claimed as evidence of Late Cenozoic exhumation of the footwall from mid-crustal depths as a result of slip on a low-angle normal fault dipping to the west.

Although this contact has been described as a normal fault plane in previous studies (with a dip of 25–30° according to Zagorchev 1992*b*, or *c.* 15–20° according to Burchfiel *et al.* 2000), it seemed to me to be more appropriately interpreted as an unconformity. The gneiss near this contact is highly weathered, the dark (biotite-rich) bands evidently more so than the light (quartzo-feldspathic) bands. Its top indeed seems to be a gradation, through progressively loose pieces of quartzo-feldspathic gneiss into a 'regolith' of fragments of this material. This is overlain by a *c.* 0.5 m thickness of poorly sorted slope wash, including clasts of granite and amphibolite, before passing into the uppermost Kalimantsi Formation. This contact is capped with gravel of inferred 'Eopleistocene' (i.e. Early Pleistocene) age, leading Zagorchev (1992*a*, 1995) to infer that slip had ended by then. Similar 'Eopleistocene' gravel was also noted by Zagorchev (1992*a*), sealing the southern part of this fault near the border with Greece (Fig. 9). However, from the evidence exposed at this roadcut site I could see no basis that it is a faulted contact at all; instead it seemed more likely that

deposition of the Kalimantsi Formation progressively buried the weathered surface of the metamorphic basement. It is clearly not an active fault, and its appearance suggests that slip on it ceased before the end of deposition of the Kalimantsi Formation. The *c.* 25–30° dip of this surface may simply indicate the profile of a weathered slope, with no relationship to the dip of any normal fault plane.

About 800 m farther NW, the contact between gneiss and Kalimantsi Formation (locally, red-weathered coarse conglomerate of rounded granite clasts) is also accessible at a lower level, *c.* 400 m a.s.l., in the Pirinska Bistritsa gorge just upstream of Gorno Spanchevo village (at [GL 09691 98880]). This contact is locally picked out by gulley erosion; the fault plane is not clearly visible, but must be steep (estimated >45° dip), because if it had a low-angle dip it would be traceable upslope to the east given the extent of local dissection of the landscape. These red-weathered sediments (of the Upper Gravel Member of the Kalimantsi Formation) are not tilted consistent with normal faulting at this margin; they instead dip at *c.* 5° towards the west, suggesting that slip on this fault had ended before they were deposited. This stratigraphic relationship can be observed in sections exposed as a result of recent incision by the Pirinska Bistritsa river, for instance at [GL 09471 97533] near Gorno Spanchevo, *c.* 1.3 km WNW of the locality in Figure 10c. Kojumdgieva *et al.* (1982) described a similar exposure *c.* 5 km farther south, where the road from Kalimantsi to Belyovo, which follows a tributary gorge of the Pirinska Bistritsa, crosses the Gorno Spanchevo Fault at *c.* 450 m a.s.l. (Fig. 10b, ii). This contact between gneiss and Kalimantsi Formation conglomerate (which I have not visited) was reported by Kojumdgieva *et al.* (1982) as a normal fault plane dipping west at *c.* 50°. However, the westward dip of this conglomerate is not apparent in Fig. 10b, ii that illustrates their interpretation of this area.

The Podgorie Fault

Just north of the border with Greece, a right bank tributary, the Strumeshnitsa, joins the Struma near Petrich (Figs 7 and 9). This tributary valley, typically *c.* 4 km wide, is bounded to the south by the *c.* 2000 m high northern escarpment of the Belasitsa mountain range. This escarpment is *c.* 60 km long (east–west), its western half being in Macedonia. This valley has formed a depocentre for sediments that have been correlated with the Sandanski and Kalimantsi Formations, these deposits now tilting to the south. This Belasitsa escarpment has been interpreted as the footwall of a significant active normal fault, the Podgorie Fault (see Zagorchev 1992*a*).

The Ograzhden Fault

Along most of the western margin of the southern Sandanski Basin the Struma follows the contact between Neogene sediments and metamorphic basement (Figs 7 and 9). This basin margin has been depicted in many studies (e.g. Zagorchev 1992*a*,*b*) as an ENE-dipping antithetic fault. Around [FL 89780 96456], beside the Struma west of Nova Delchevo, the basement surface (interpreted as a gently basinward-sloping erosion surface of Mid-Miocene age; see Zagorchev 1992*a*,*b*, 1995) steepens at the basin margin to produce an escarpment up to *c.* 50 m high. Zagorchev (1992*a*) estimated the total slip on this fault as *c.* 500 m, of which *c.* 50–100 m was considered post-Pliocene. However, this escarpment is not particularly fresh-looking, and its height is less than the >100 m by which the Struma, which flows at its base, is estimated to have incised since the Early Pleistocene (see below). It is thus possible that this escarpment has been formed by recent fluvial erosion, or is an inactive fault line scarp exposed by this fluvial incision, rather than indicating an active antithetic normal fault with a very low slip rate.

This locality also provides clear exposures of the silt and tuffite of the Delchevo Formation, locally dipping at up to 25° towards N52°E. This disposition confirms that the main normal faulting affecting this basin has occurred along its eastern, or ENE, margin. The presence of these fine-grained sediments beside the Ograzhden Fault suggests that this fault was not yet active at the time, consistent with a later start of local extension, a view reinforced by the pockets of similar sediment on the eastern flank of the Ograzhden Massif in the footwall of this fault (see Kojumdgieva *et al.* 1982; Fig. 9).

Interpretations of low-angle normal faulting

Burchfiel *et al.* (2000) used evidence from the Sandanski Graben to infer large-scale extension in the Mid–Late Miocene. With regard to Ilindentsi, they wrote (pp. 332–333): 'A prominent layer of limestone breccia [was] emplaced in Pontian time ... Limestones similar to those within the breccia ... are not present directly east of the Sandanski Graben and probably have a source many kilometres to the east. This suggests that the normal faults that bound the east side of the Sandanski Basin have many kilometres

of Middle–Late Miocene displacement.' These remarks are problematic; as well as being clear in the field (Fig. 10a), it is evident from geological maps (Marinova & Zagorchev 1990; Zagorchev & Dinkova 1990) and the local literature (e.g. Nedjalkov *et al.* 1986; Zagorchev 1992*a*, 1995, 2001*a*) that the Dobrostan Marble directly upslope from Ilindentsi was the source of the marble clasts Ilindentsi Member of the Kalimantsi Formation. Rather than requiring many kilometres of normal slip, the close proximity of source area and depocentre preclude this.

In describing the Gorno Spanchevo Fault, Burchfiel *et al.* (2000) wrote (p. 333) 'the basin is bounded by a gently (*c.* 15–20°) west dipping normal fault that juxtaposes Middle Miocene sediments ... against ... basement of the Rhodope Massif ... Slickensides ... indicate an east-northeast–west-southwest direction of extension.' It is not clear how they identified slickensides; none were evident to me. Nor is it clear how they interpreted Middle Miocene sediment juxtaposed against basement, as the available mapping (e.g. Kojumdgieva *et al.* 1982; Zagorchev 1992*a*, 1995; Fig. 9) shows the uppermost Kalimantsi Formation in contact with basement throughout this structure.

The Razlog and Gotse Delchev Basins

The Razlog and Gotse Delchev Basins are east of the the Rila and Pirin Massifs and are thus drained by the Mesta River (Fig. 7). They both cover part of the larger Palaeogene Mesta Basin (see Zagorchev 1995; Burchfiel *et al.* 2003), and the same stratigraphic terms are used for both these basins). The designated Neogene sequence begins with the Valevitsa Formation (basal conglomerate and sandstone). This is overlain by the Baldevo Formation, comprising interbedded siltstone, silty clay, fine sandstone, diatomite and lignite, in turn overlain by the Nevrokop Formation of fluvial conglomerate and sandstone (see Vatsev 1980). The Valevitsa Formation has yielded pollen of Pontian age (e.g. Vatsev 1980), and the Baldevo Formation has yielded Pontian plant remains (e.g. Palmarev 1970; Ivanov 1995) and diatoms (e.g. Temniskova & Ognjanova 1983) but its upper part has yielded algae of inferred Pliocene age (Zagorchev 1995). Conglomerates of the Nevrokop Formation, unlike those in the older formations, contain clasts of Palaeogene granite from the Pirin Massif (from the Teshovo and Central Pirin plutons), suggesting that it postdates their unroofing and thus correlates with the Kalimantsi Formation of the Sandanski Basin (Zagorchev 1995).

At Hadzhidimovo, the lower Nevrokop Formation has yielded characteristic Turolian mammals, including the hipparion *Cremohipparion mediterraneum*, the antelope *Paleoreas lindenmayeri*, and the four-tusked elephant *Tetralophodon longirostris* (Nikolov 1985). These species all spanned biozones MN11–13 (see Bernor *et al.* 1996; Gentry & Heizmann 1996; Lungu & Obada 2001). Zagorchev (1995) inferred a Pontian age (MN13; 7.1–5.4 Ma) for this site, whereas Geraads *et al.* (2001) placed it in early MN12 (*c.* 8.2–7.1 Ma). At Borovo, the upper Nevrokop Formation has yielded the mastodon *Anancus arvernensis* (see Nikolov 1985). Zagorchev (1995) considered this stratigraphic level to be Early Pliocene (Ruscinian), but this was a long-lived species spanning biozones MN14 to MN17 (i.e. the whole Pliocene) (see Athanassiou & Kostopoulos 2001; Lungu & Obada 2001) so it provides no strong constraint on the end of deposition. After sedimentation ceased (before the Early Pleistocene), the Mesta began to incise into the basin floor, forming a staircase of river terraces (see Nenov *et al.* 1972).

Several studies (e.g. Ivanov 1995; Zagorchev 1995) have suggested that the three 'Formations' defined for the Gotse Delchev Basin interfinger with each other or pass laterally into each other, indicating a lateral facies variation from typical coarser sediment in the west adjacent to the sediment source in the Pirin Massif to finer sediment in more distal localities. The overlap in dates between sites assigned to the Baldevo and Nevrokop Formations (noted above) would seem to confirm this.

The Razlog Basin has an irregular shape (Fig. 7); only its SSW margin appears to be bounded by a major normal fault (the Predela Fault; see below), elsewhere, the eroded margins of its Neogene sequence appear to lap onto Eocene terrestrial sediments of the Mesta Basin and older metamorphic basement. The Gotse Delchev Basin is more regular, *c.* 25 km long (north–south) and *c.* 8 km wide. However, many studies (e.g. Nenov *et al.* 1972; Ivanov 1995) have noted that its depocentre is typically not normal fault bounded: these sediments instead lap onto the basement at the basin margins. The maximum overall thickness of the Neogene deposits in this basin is *c.* 600 m (e.g. Ivanov 1995; Zagorchev 1995), rather less than in the Sandanski Basin.

The Predela Fault

This fault (named by Zagorchev 1995; Meyer *et al.* 2002 called it the Bansko Fault) bounds

the southern margin of the Razlog Basin, with typical N70°W strike. Its *c.* 800 m high footwall escarpment, rising to *c.* 2100 m a.s.l., is prominent in the field (Fig. 7) and on satellite images (Meyer *et al.* 2002). Its overall along-strike length is *c.* 30 km (see Meyer *et al.* 2002); its hanging wall forms the Predela col between the Pirin and Rila massifs; its western end adjoins the eastern end of the Krupnik Fault (see above).

South of Bansko (Fig. 7), the moraine of an ice lobe emanating NE from Mt Vihren can be seen to be offset *c.* 10 m by this fault. As well as proving its Holocene activity and indicating a slip rate approaching 1 mm a^{-1}, this locality thus provides a rare instance of interaction between glaciation and active normal faulting in the Aegean region.

The Gotse Delchev Fault

No clear normal fault escarpment bounds the eastern margin and much of the western margin of the Gotse Delchev Basin. The clearest instance where its western margin is normal fault bounded is between Gotse Delchev and Musomishta. Here, as documented by Zagorchev (1995), two N60°W-striking normal faults are arranged en echelon: the Musomishta Fault, dipping NNE at *c.* 50–70° and with a *c.* 300 m high footwall escarpment, forms the contact between the Nevrokop Formation in its hanging wall and the Dobrostan Marble in its footwall. Approximately 1 km farther NNE, the subparallel Gotse Delchev fault offsets the Nevrokop Formation, with a *c.* 100 m high footwall escarpment (Fig. 7). The fresh appearance of this escarpment (for instance at [GM 29891 05108], *c.* 1 km south of Gotse Delchev town), including characteristic faceted spurs and incised wineglass canyons, suggests that this normal fault is active, especially as the sediment exposed in this uplifting footwall is not fully lithified; this faulting clearly post-dates the deposition of this sediment.

Discussion

Correlations between sedimentary sequences

Figure 11 indicates schematically how the sedimentary sequences in different basins in SW Bulgaria correlate. Its main differences compared with similar diagrams published previously (e.g. Burchfiel *et al.* 2000, fig. 6; Zagorchev 2001*a*, fig. 15) are the adoption of a clear time scale and the placing of the Meiotian–Pontian boundary for the Paratethyan realm at the Tortonian–Messinian boundary, consistent with most modern quantitative chronostratigraphies (e.g. Steininger *et al.* 1996).

One clear feature shown is the ending of sedimentation in all basins at *c.* 3 Ma. Since this time, with minor exceptions this part of Bulgaria has been subject to erosion, with stacked depositional sequences no longer developing. The principal exception is the stacked Late Pliocene–Pleistocene sedimentation south and west of Sofia, around Radomir and Trun (Fig. 2). This part of Bulgaria is at the drainage divide between the south-flowing Struma, the Ishkur that flows NE from the Sofia area to the Danube, and the Nishava that flows northwestward across Serbia to the Morava, then northward to the Danube; being in headwaters, where rivers have little erosional power, this area has not experienced the hundreds of metres of recent fluvial incision typical elsewhere.

This synchronous ending of sedimentation was previously noted by Zagorchev (2001*a*), although he assigned it a nominal age of *c.* 2 Ma rather than *c.* 3 Ma. It differs from the depiction by Burchfiel *et al.* (2000), who inferred (without providing supporting evidence) different timings for the cessation of sedimentation in different basins. As is clear from the descriptions above, this ending of sedimentation is not precisely dated in any basin, but there is no basis for assigning it a different age in different basins. As is discussed in more detail below, a nominal age of *c.* 3 Ma, rather than *c.* 2 Ma, is favoured for this event here, to match the Late Pliocene fluvial incision that is widely observed across western and central Europe (see Westaway 2002*a*).

The observation that the extensional region of SW Bulgaria is almost entirely erosional marks one clear difference relative to western Turkey, where the hanging walls of the principal onshore active normal faults (bounding the Alaşehir and Büyük Menderes grabens; Fig. 1a) are active depocentres. In both western Turkey and SW Bulgaria, vertical crustal motions caused by active normal faulting are superimposed onto regional uplift at comparable rates (see, e.g. Westaway *et al.* 2004; also below, where the regional uplift rate in SW Bulgaria is estimated as *c.* 0.15 mm a^{-1}). This difference presumably relates to slower extension in SW Bulgaria. Extension rates are estimated below as no more than *c.* 1 mm a^{-1} on any of the active normal faults in SW Bulgaria. Assuming a 45° dip, 1 mm a^{-1} of slip on a normal fault in an erosional region could be partitioned with 90% footwall uplift and 10% hanging-wall subsidence relative to the uplifting regional reference frame. So, with regional uplift at *c.* 0.15 mm a^{-1}, the footwall and hanging wall would uplift at 1.05 mm a^{-1}

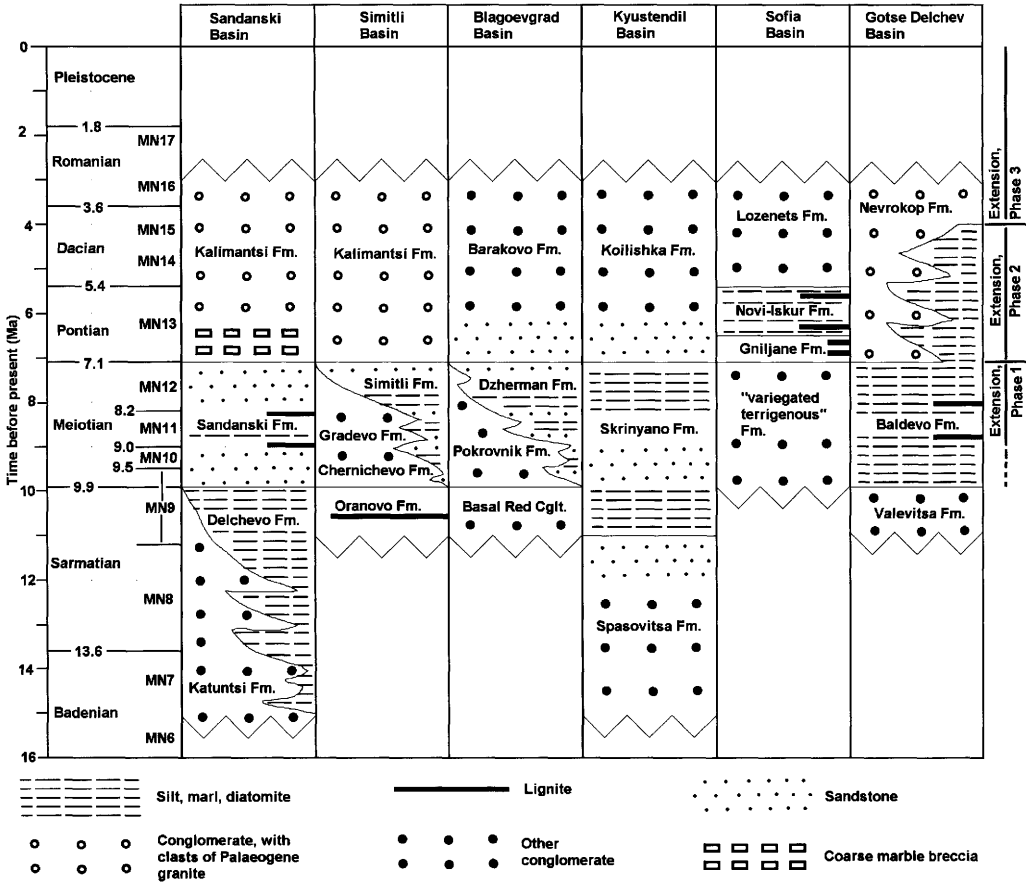

Fig. 11. Stratigraphic correlation diagram for the Late Cenozoic terrestrial sedimentary basins of SW Bulgaria. Slope deposits and river terraces are omitted. Sources of information for most of these basins are discussed in the text. The stratigraphy for the Sofia Basin is from Kamenov & Kojumdgieva (1983), with mammalian biostratigraphic control from Nikolov (1985). The stratigraphy for the Kyustendil Basin is from Vatsev & Bonev (1994), also with mammalian biostratigraphic control from Nikolov (1985). As noted in the text, the Katuntsi Formation of the Sandanski Basin is problematical; it may be indistinguishable from the Kalimantsi Formation (see Kojumdgieva *et al.* 1982). The age bounds for the terrestrial Paratethyan stages and mammalian biozones, which are constrained by magnetostratigraphy and Ar–Ar dating, are from Steininger *et al.* (1996), and are thus unaffected by the revision of the 'marine' Paratethyan chronology proposed by Vasiliev *et al.* (2004).

and 0.05 mm a^{-1}, respectively. In contrast, using geodetic data from McClusky *et al.* (2000), Westaway *et al.* (2004) estimated the extension rate across the Alaşehir graben as *c.* 6 mm a^{-1}, superimposed onto regional uplift at *c.*0.2 mm a^{-1}. Partitioning the normal fault-related vertical motions as before would now indicate absolute hanging-wall subsidence. However, on other, less active, normal faults in western Turkey, hanging walls are experiencing absolute uplift (e.g. Westaway 1993; Purvis & Robertson, 2004; Westaway *et al.* 2004, 2005), as in SW Bulgaria.

In contrast, the starts of sedimentation differ widely between basins. Several sequences start with thin basal conglomerates that seem to have accumulated slowly over long periods of time before sedimentation rates increased significantly; others begin with stacked sequences of silt (the Delchevo Formation in the Sandanski Basin) or lignite (the Oranovo Formation of the Simitli Basin). Although a general coarsening upward is apparent (Fig. 11), some sequences are dominated by clastic input, whereas others, notably in the Gotse Delchev and Sofia basins, were

lacustrine basins, where rhythmic alternations of deposition of lignite, diatomite and other sediments indicate fluctuations in environmental conditions.

Thorough high-resolution chronostratigraphic studies have been carried out in the apparently analogous rhythmic Messinian–Early Pliocene sequence in the Servia–Ptolemais Basin of NW Greece (Fig. 1a) (e.g. van Vugt *et al.* 1998, 2001; Steenbrink *et al.* 1999, 2000). These studies indicate Milankovitch forcing of the sedimentary rhythmicity, under the dominant influence of *c.* 20 ka precession cyclicity, with lignite deposition at times of cool summers (i.e. summer insolation minima, when the Earth's orbit was oriented with aphelion during the northern hemisphere summer) and marl or diatomite deposition at times of warmer summers. This implies that palaeo-lakes were typically deeper when summers were warmer, implying higher summer precipitation, as is generally accepted for the northern margin of the eastern Mediterranean (e.g. Rohling & Hilgen 1991). Rhythmicity in the Bulgarian lacustrine sequences has instead been explained in terms of alternations between 'silting up', marked by lignite deposition, and renewed subsidence, marked by deepening of water and deposition of diatomite (e.g. Ognjanova & Yaneva 2001). These Bulgarian lake basins would be good targets for future high-resolution cyclostratigraphic studies.

Structural and geodetic estimates of slip rates for the present phase of extension

This description indicates that the principal active normal faults in SW Bulgaria strike west (between WSW and NW; Figs 3, 7 and 9). If this region accommodates uniaxial extension on these faults, then the extension direction is roughly north–south. This set of subparallel, en echelon normal faults continues farther north, a notable additional member being the north-dipping Sofia fault (Fig. 2), whose footwall forms the *c.* 1200 m high northern escarpment, rising from *c.* 700 m to *c.* 1900 m a.s.l., of the Vitosha mountain range south of Sofia. Burchfiel *et al.* (2000) regarded the Sofia Basin as effectively marking the northern limit of the Aegean extensional province.

Figure 1b illustrates the crustal velocity field in SW Bulgaria, measured by Kotzev *et al.* (2001) using the Global Positioning System (GPS). GPS point BERK, north of the Sofia Basin (Fig. 2), is the most southerly site in stable Eurasia, delimiting the northern margin of the Aegean extensional province. The progressive increase in southward velocity that is observed geodetically to occur southward from this point is evidently the result of the cumulative slip on the various east–west-striking normal faults in the region, including the Sofia, Kyustendil, Saparevo, Rila, Krupnik, Predela, Podgorie and Gotse Delchev faults. The cumulative extension across this array of en echelon normal faults can thus be estimated to account for the observed (Fig. 1b) *c.* 3 mm a^{-1} of southward motion of the southern margin of western Bulgaria relative to stable Eurasia. Rates of southward motion increase dramatically farther south across Greece, as illustrated by the velocity vector at SOXO in Figure 1b and by the data presented by McClusky *et al.* (2000, fig. 2).

Taking account of the heights and dips of footwall escarpments and the thicknesses of hanging-wall fill, the most important active normal faults in this array can be estimated to have taken up 2–3 km of extension. As a result, the total extension along a north–south line across the Sofia, Saparevo, Krupnik and Podgorie faults can be estimated as *c.* 10 km. Dividing this into the geodetic extension rate gives an estimated age of this phase of faulting of 3–4 Ma. As already noted, the start of this phase of extension is not well constrained directly, largely because of the uncertainties over dating the Pliocene sediments in the region. Burchfiel *et al.* (2000) estimated a similar (*c.* 3.5–4 Ma) timing of the start of this phase of extension, but this seems to have been based on arguments regarding a preceding phase of hypothetical low-angle normal faulting (see Dinter & Royden 1993), which no longer appear appropriate (see below); its agreement with the numerical age estimate in the present study may be coincidental.

Recent syntheses (Westaway 2003, 2004*a*) place the start of the present phase of right-lateral slip on the North Anatolian Fault Zone (Fig. 1a), during which it has been conjugate to the left-lateral East Anatolian Fault Zone (EAFZ), around 4 Ma. The NAFZ is estimated in these schemes to have first developed around 7 Ma, but was initially conjugate to the left-lateral Malatya–Ovacık Fault Zone (MOFZ) located north of the modern EAFZ. During these two phases of slip, the Euler pole to the NAFZ seems to have been located in different places (see Westaway 2004*b*), so one may well expect the kinematics of regions near its western end to have changed significantly around 4 Ma.

Constraints on the earlier extension

In the Burchfiel *et al.* (2000) scheme, extension is presumed to have begun in the southern Sandanski Basin in the early Badenian stage of

the Mid-Miocene (*c.* 15 Ma), the deposits of the Delchevo Formation being presumed by them to be synextensional. This phase of extension was considered to be oriented NE–SW, by analogy with apparent synchronous low-angle normal faulting in northern Greece (see Dinter & Royden 1993; Dinter *et al.* 1995). Burchfiel *et al.* (2000) deduced that the zone of extension expanded in the Early Meiotian (*c.* 9 Ma) to affect the whole Sandanski Basin, the Blagoevgrad, Gotse Delchev, Razlog and Sofia basins, and other basins located outside the present study region. However, as already noted there is no direct evidence that the Delchevo Formation was deposited during crustal extension, and some evidence that it was not.

The Delchevo Formation is tilted eastward at up to 25° (see above). From Zagorchev & Dinkova (1990), the Sandanski Formation dips at up to 25° near its base and typically at 10–15° near its top (Fig. 9), whereas the Kalimantsi Formation typically dips at up to *c.* 10° near its base but can be subhorizontal at its top. The similarity in tilt between the Delchevo Formation and the lower Sandanski Formation suggests that extension began early during deposition of the latter.

Evidence already discussed (e.g. Fig. 10c and d) suggests that the end of slip on the Gorno Spanchevo Fault preceded the end of deposition of the Kalimantsi Formation. The fluvial gravels of inferred 'Eopleistocene' age, which 'seal' the normal faults at the eastern margin of the Sandanski Basin, confirm that these faults ceased to be active before the Early Pleistocene. Zagorchev (1992*a*) suggested an alternative explanation: that so much extension occurred on the Gorno Spanchevo Fault that it became back-tilted to such an extent that it was no longer suitably oriented relative to the stress field, so the Melnik Fault formed in its hanging wall with a steeper dip. This adjustment process is observed in many parts of the Aegean region that have extended significantly, such as along the Alaşehir and Büyük Menderes fault zones in western Turkey (e.g. Westaway 1998; Purvis & Robertson 2004). However, from Zagorchev's (1992*a*) estimate, the heave across the West Pirin Fault is only moderate, at most *c.* 3.5 km × cot(50°) or *c.* 3 km. It is unlikely to have been much greater at the southern end of the Sandanski Basin, so severe back-tilting on any normal fault seems unlikely. Slip on this set of faults is now presumed to have ended by *c.* 4 Ma given the timing of the start of the younger phase that superseded it (see above). This normal fault system, oriented NNW–SSE, was thus unsuited to take up NNW–SSE extension when this began at *c.* 4 Ma.

Regional kinematics

The evidence suggests that three distinct phases of extension have occurred in SW Bulgaria from the Late Miocene to the present day. The start of sedimentation in several basins (Fig. 11) suggests that in each case local extension began in the early Meiotian stage of the Late Miocene. Extension at this time is presumed to have been towards the WSW or SW, accommodated on NNW–SSE-striking normal faults, such as the West Rila (Fig. 3) and West Pirin (Figs 7 and 9) faults. This timing matches the earliest evidence for the 'present' phase of extension in NW Turkey from this region's earliest alkali basaltic volcanism, which is dated to *c.* 10 Ma in the Tekirdağ and Çanakkale areas (Fig. 1a) in the vicinity of the modern Sea of Marmara (see review of this dating evidence by Westaway *et al.* 2005). At this time, the Sea of Marmara itself did not exist, because the NAFZ had not yet developed. Moreover, before the subsequent many tens of kilometres of right-lateral slip accumulated on the NAFZ, Tekirdağ and Çanakkale would have been closely juxtaposed. At this time, it thus appears that extension may have affected only a limited part of the present Aegean region, in NW Turkey and southern Bulgaria (Fig. 12b). It is suggested that this initial phase of extension was caused by incipient 'rollback' of the oceanic slab that was subducting beneath the southern margin of the Aegean region; beforehand, it is presumed that the downdip length of this slab was insufficient to drive this process (Fig. 12a).

As noted above, it is inferred that the various pre-Meiotian sedimentary deposits in SW Bulgaria (Fig. 11) are not extension related. Some of these deposits (e.g. the Oranovo Formation) are localized, and the depocentre of the Delchevo Formation was evidently cut through by later normal faulting. It thus evident that when active normal faults began to develop in this region some of them cut through pre-existing depocentres that existed for other reasons. Such a geometry, of sediments accumulating in depocentres that are unrelated to normal faulting, but that later become overlain by hanging-wall sedimentary fill, is widely observed in western Turkey (e.g. Koçyiğit *et al.* 1999; Bozkurt 2000; Yılmaz *et al.* 2000). It has indeed caused many problems with trying to date the start of extension, as studies (e.g. Seyitoğlu & Scott 1992; Seyitoğlu *et al.* 1992) have regarded this older sediment as part of the synextensional sequence, causing the start of extension to be placed too early in the record. By analogy, it seems likely that the start of extension in SW Bulgaria was no earlier than the Meiotian.

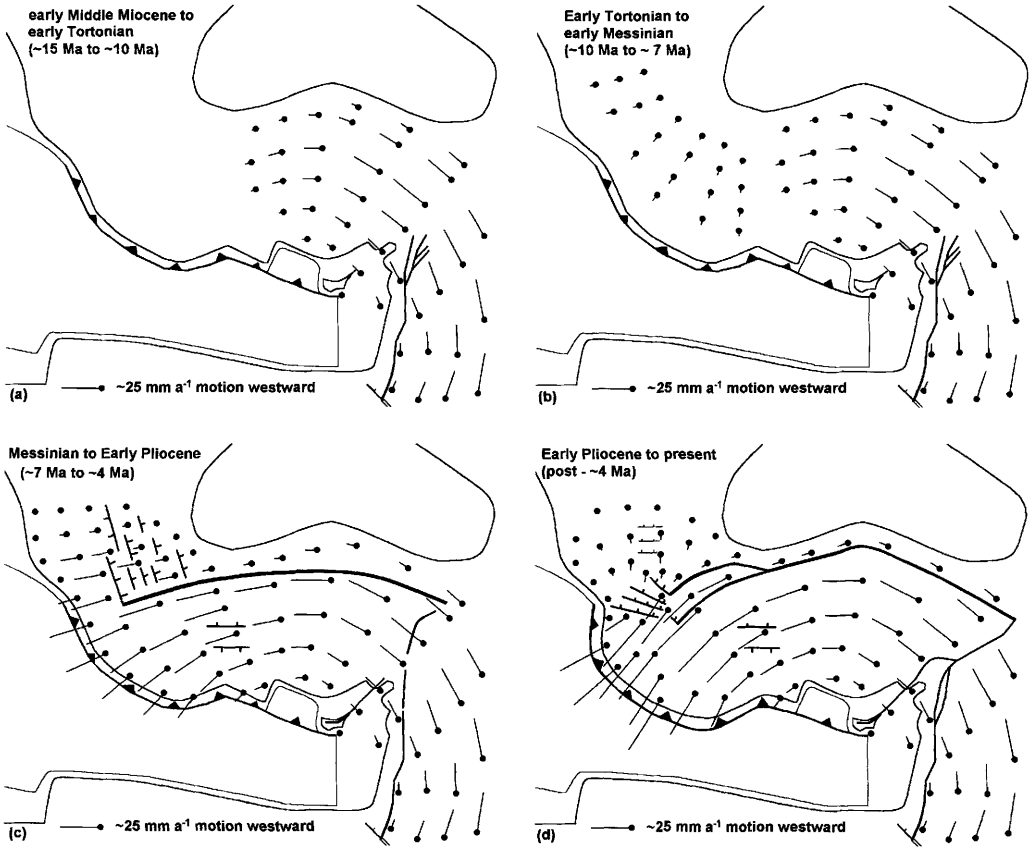

Fig. 12. Schematic crustal velocity fields at key stages in the evolution of the Aegean region during the Late Cenozoic, consistent with the present study. (**a**) In the Mid-Miocene, with no extension yet occurring in the Aegean region. Northward relative motion of the Arabian plate relative to Africa and Eurasia was already occurring, but the Dead Sea Fault Zone died out into a complex zone of transpression in Syria and SE Turkey and a broad zone of distributed shortening in eastern and central Turkey (see Westaway 2003, 2004*a*). (**b**) In the early Late Miocene, with slow extension inferred in parts of NW Turkey (from volcanism; see Westaway *et al.* 2005) and analysis of SW Bulgaria (this study). (**c**) The deformation accompanying the initial phase of NAFZ slip, during *c.* 7–4 Ma, accommodated by NNW tapering of WSW extension across Bulgaria. The timing of this phase is constrained by arguments in the main text. Velocities during this phase have been scaled to the same rate of relative motion between the Turkish plate and Eurasia as at present (see McClusky *et al.* 2000), although as discussed in the text the typical contemporaneous velocities may have been lower. (**d**) The deformation accompanying the present phase of NAFZ slip, since *c.* 4 Ma, accommodated by southward extension across Bulgaria and by westward tapering of southward extension across central Greece. This velocity field is essentially a schematic version of the results of McClusky *et al.* (2000). Their results are well known to be consistent with the NAFZ kinematics; they have been shown by Westaway (2003, 2004*a*) to be consistent with the active strike-slip faulting in SE Turkey; and are now shown to also be consistent with the active faulting in Bulgaria. (See text for discussion.)

In the Early Pontian (*c.* 7 Ma), extension in SW Bulgaria seems to have spread more widely (for instance, the deposition of the lacustrine Gniljane Formation suggests that extension began at this time in the Sofia Basin; Fig. 11). This effect was noted by Burchfiel *et al.* (2000), who inferred much more widespread extension in the Pontian (their fig. 9) than in the Meiotian (their fig. 8). Extension also evidently spread westward, as indicated by the 6.9 Ma start of lacustrine deposition (Steenbrink *et al.* 2000) in the Servia–Ptolemais basin of northern Greece (Fig. 1a). The typical coarsening of the sediment at this time in the depocentres of SW Bulgaria

(Fig. 11) also suggests a higher-energy environment, with faster erosion in footwall localities, implying an increase in structural relief and thus in slip rates (see Zagorchev 1992*a*). However, this time marked the onset of the Messinian salinity crisis in the Mediterranean region, so some change in sedimentary environments may reflect contemporaneous climate change (for instance, increased aridity may have reduced the vegetation cover, leading to increased rates of erosion). However, it seems obvious that the emplacement at this time of the marble olistostromes of the Ilindentsi Member of the Kalimantsi Formation in the Sandanski Graben required significant local topographic gradients for the first time, from which it can be inferred that the footwall of the West Pirin normal fault was uplifting at a significant rate relative to the adjacent hanging wall. At this time, extension in SW Bulgaria seems to have continued, as before, in the ENE–SSW direction.

Recent interpretations (Westaway 2003, 2004*a*; Westaway *et al.* 2005) regard *c.* 7 Ma as a key point in the tectonic evolution of Turkey, marking the starts of the initial phase of slip on the NAFZ (conjugate to the MOFZ in the east; see Westaway & Arger 1996, 2001) and of the 'present' phase of north–south extension across most of western Turkey. Robertson *et al.* (2004) also deduced a *c.* 7 Ma switch from crustal shortening to strike-slip in the NE corner of the Mediterranean Sea, in good agreement with these estimates. As discussed by Westaway. (2006), the clearest evidence now available for this timing of extension in western Turkey has been developed from the dating to *c.* 6.7 Ma of the extension-related volcanism in the Denizli region (see Westaway *et al.* 2005) and from thermochronological evidence (from Lips *et al.* 2001) indicating a *c.* 7 Ma start of rapid slip on normal faults bounding the Alaşehir graben (Fig. 1a). Westaway (2003, 2004*a*) has suggested that the start of this phase of extension was synkinematic with the start of slip on the NAFZ, both processes having possibly been triggered by the change in state of stress in the crust that accompanied the drawdown in sea level in the Mediterranean basin at the start of the Messinian salinity crisis (see calculations by Westaway 2003). It follows that, at this time, coupling via the right-lateral slip on the NAFZ for the first time caused kinematic linkage between the pre-existing convergent zone in eastern Turkey (Fig. 12a and b) and the Aegean extensional province (Fig. 12c).

Finally, at a later stage, estimated above as *c.* 4 Ma, the extension in SW Bulgaria changed from ENE–WSW to NNW–SSE or north–south (Fig. 12d). The major NNW–SSE-striking normal faults in this region, such as the West Rila and West Pirin faults, were no longer suitably oriented to accommodate the extension, and became superseded by more optimally oriented normal faults, such as the Kyustendil, Rila, Krupnik and Podgorie faults. However, some pre-existing normal faults that were oblique to the earlier ENE–WSW extension were evidently also oblique to the subsequent NNW–SSE extension, and so could remain active; these include the Sofia, Saparevo, Predela and Musomishta faults (Figs 3 and 7). This array of roughly west–east-striking active normal faults seems to persist southward into northern Greece: similarly oriented faults there bound the Langadas graben (having slipped in the $M=6.4$ Thessaloniki earthquake sequence in 1978, accommodating north–south extension; Soufleris *et al.* 1982; Tranos *et al.* 2003) as well as the Serrai, Drama, and Xanthi grabens (Fig. 1a). The $M=6.6$ Grevena earthquake sequence in 1995, farther west in northern Greece (Fig. 1a), also involved north–south extension (e.g. Rigo *et al.* 2004). By analogy, the poorly documented Plovdiv (Fig. 2) earthquake sequence in central Bulgaria in 1928 (mainshock $M=7$; see Richter 1958) probably also involved north–south extension.

This estimated *c.* 4 Ma timing corresponds to the end of slip on the MOFZ, when the NAFZ propagated eastward and the EAFZ developed conjugate to it (see Westaway & Arger 1996, 2001; Westaway 2003, 2004*a*). Its timing is estimated by dividing the total slip on the EAFZ by its slip rate; Westaway *et al.* (2006) have constrained this timing to 3.73 ± 0.05 Ma by this method. As Westaway (2004*b*) noted, it is difficult to make predictions for how the NAFZ behaved before this time, because of the possibility that the Euler vector for the motion relative to Eurasia of the Turkish plate to the south of it may have differed for its two phases of slip. At present, this Euler pole is located near the SE corner of the Mediterranean Sea near the Suez Canal (see McClusky *et al.* 2000). If during the previous phase it was several hundred kilometres farther south and west, making it more distant from the NAFZ, the resulting adjustment in deformation sense can explain the change in the extension direction in SW Bulgaria (Fig. 12c and d).

Recent studies of the Sea of Marmara pull-apart basin, where, during its present slip phase, the main active strand of the NAFZ steps to the right (Fig. 1a), shed some light on the duration of its present geometry. Localized right-lateral slip occurs on the NAFZ at a rate of 18 ± 4 mm a^{-1} (Hubert-Ferrari *et al.* 2002). Probably 80% of this, or *c.* 15 mm a^{-1}, is taken up across the Sea

of Marmara, the rest occurring on subparallel strands farther south (Fig. 1a; see Armijo *et al.* 1999). Armijo *et al.* (1999) estimated that this northern NAFZ strand has slipped by *c.* 60 km since its present geometry developed, which would suggest initiation at *c.* 60/*c.* 15 or *c.* 4 Ma. However, using different reasoning, Okay *et al.* (2004) obtained a revised lower bound to its estimated slip of *c.* 40 km, whereas using a different argument Seeber *et al.* (2004) estimated that it has slipped no more than 28 km. Attempts to date the start of this slip directly using local sedimentary evidence have led to further controversy, because the ages of the sedimentary units and their relationships to this faulting have been disputed (see Tüysüz *et al.* 1998; Armijo *et al.* 1999; Yaltırak *et al.* 2000). It is thus clear that no consensus yet exists regarding which local evidence provides the best estimate of the start of the present phase of NAFZ slip, but an age of *c.* 4 Ma cannot be precluded.

The present geometry (Fig. 12d) achieves kinematic consistency between the slow southward or SSW velocities (at *c.* <10 mm a^{-1}) that develop across Bulgaria and northern Greece and the 35–40 mm a^{-1} SSW velocities observed south of the western end of the NAFZ (see McClusky *et al.* 2000; Kotzev *et al.* 2001). Such consistency requires rapid southward or SSW extension across the en echelon set of major active normal faults in central Greece, including the faults bounding the Gulf of Corinth, the Parnassos mountain range, the Sperchios basin and adjacent Gulf of Evvia, the north coast of Evvia, and the SE end of the Thermaic Gulf and SW end of the North Aegean Trough (Fig. 1a). The required extension rate increases eastward from zero in the west to *c.* 25–30 mm a^{-1} along a line between the eastern Gulf of Corinth and the intersection between the Thermaic Gulf and North Aegean Trough. This westward tapering in extension rates will require clockwise rotation of the Peloponnese block to the south (Fig. 1a) relative to regions farther north. The importance of the active normal faulting in this region for maintaining kinematic consistency between Aegean extension and right-lateral slip on the NAFZ, and for generating clockwise rotations that are observed palaeomagnetically, was recognized long ago (e.g. McKenzie & Jackson 1983). However, in their scheme the normal-fault-bounded blocks were envisaged as like slats attached to pivots at both ends, which means that the predicted extension and rotation do not vary laterally. In contrast, the present scheme resembles the opening of a fan about a pivot in the west, with extension increasing from west to east and clockwise rotation increasing from north to south.

Between *c.* 7 and *c.* 4 Ma the right-lateral slip on the NAFZ is inferred to have been accommodated by NNW tapering in the SSW extension across Bulgaria (Fig. 12c). This geometry would also result in clockwise rotation, which would have increased from east to west; it indeed resembles the 'classic' geometrical interpretation of such palaeomagnetic evidence for the western Aegean region (see Kissel & Laj 1988). The observed palaeomagnetic dataset indicating systematic clockwise rotation across the western half of this extensional province (see Kissel & Laj 1988) would thus appear to relate in part to each of the deformation senses in Figure 12c and d, rather than requiring a single mechanism. In contrast, in western Turkey the crustal velocity field is predicted to have remained essentially the same after 4 Ma as before (Fig. 12c and d), consistent with the absence of evidence for a change in the deformation sense at this time.

During the initial phase of NAFZ slip, the geometry (Fig. 12c) suggests that the NAFZ slip rate should equal the maximum rate of WSW extension along a line directly north of the NAFZ and the maximum rate of WSW rollback (relative to Eurasia) of the surface trace of the Hellenic subduction zone. In contrast, during the present phase, the maximum rate of SSW extension across Bulgaria and northern Greece plus the NAFZ slip rate should roughly equal the maximum rate of WSW rollback (relative to Eurasia) of the surface trace of the Hellenic subduction zone. From two points of view the present deformation sense can be considered more 'effective' than its predecessor. First, it allows faster rollback of the Hellenic subduction zone for a given NAFZ slip rate. As the length of subducted slab increases, the dynamics favours faster rollback (see Meijer & Wortel 1997), potentially forcing this change in deformation sense as a mechanically 'easier' alternative than forcing a faster NAFZ slip rate. Second, the geometry in Figure 12d avoids the requirement in Figure 12c for rapid ENE–WSW crustal shortening north of the western end of the subduction zone. Such shortening would lead to crustal thickening and, thus, growth of topography, affecting the regional stress field so as to ultimately oppose the driving mechanism. However, detailed calculations regarding both these potential causes of the *c.* 4 Ma reorganization of the kinematics are beyond the scope of this study.

Local versus regional vertical crustal motions

Across most of the Aegean region, the view became established in the 1980s (see Jackson

et al. 1982; Jackson & McKenzie 1988) that vertical crustal motions during extension have been caused only by active normal faulting. This is despite an abundance of evidence to the contrary, notably from Turkey, for regional uplift, onto which local effects of active normal faulting have been superimposed (see summary of this evidence by Demir *et al.* 2004). It is now clear that *c.* 400 m is a representative typical value for the regional uplift in western Turkey since the Early Pliocene, of which *c.* 150 m has occurred since the start of the Mid-Pleistocene (see Westaway 1993; Westaway *et al.* 2003, 2004). The early Mid-Pleistocene marked a general increase in uplift rates at localities in temperate latitudes worldwide (e.g. Kukla 1975, 1978; Westaway 2002*a*), apparently linked to coupling between surface processes (e.g. increased erosion rates, cyclic loading by ice sheets) caused by long time-scale climate change (as the climate system adjusted from predominant *c.* 40 ka to *c.* 100 ka climate cyclicity; see Mudelsee & Schulz 1997) and the isostatic uplift response that is mediated by flow in the lower continental crust. An apparently similar increase in uplift rates also occurred around 3 Ma (see van den Berg & van Hoof 2001; Westaway 2001, 2002*a*), but is less well resolved because of the more limited datasets from that time. However, despite the evidence to the contrary, other studies (e.g. Bunbury *et al.* 2001) continue to repeat the view that vertical crustal motions in western Turkey relate only to active normal faulting. The recent publication (by Allen *et al.* 2004*a*) of the extraordinary claim that there is no evidence of uplift in Turkey since the Miocene provoked a strong reaction (Westaway 2004*b*) but even so was not retracted (Allen *et al.* 2004*b*).

Given this history of dispute in western Turkey, it is noteworthy that it is well established that in SW Bulgaria local vertical crustal motions as a result of Late Cenozoic normal faulting have been superimposed onto regional uplift (e.g. Zagorchev 1992*a*,*b*). The local literature indeed contains extensive discussion of erosion surfaces in the mountain massifs, which have been warped and offset by normal faulting and dissected to progressively lower levels by fluvial incision in response to this regional uplift.

The youngest part of this history of regional uplift is revealed by the terrace staircases of the Struma and Mesta rivers (Table 1), which are well developed in the Sandanski and Gotse Delchev basins and elsewhere. These terraces seem to correlate well with the principal cold stages from the latest Early Pleistocene (oxygen isotope stage (OIS) 22; Shackleton *et al.* 1990) to the Late Pleistocene. These terrace staircases thus resemble those of the major rivers in Turkey (see Demir *et al.* 2004), but differ from those in central and western Europe where often every cold stage is represented, sometimes with multiple terraces per climate cycle (e.g. Westaway 2002*a*). Of the two, the Struma terrace staircase is taken as a better proxy for regional uplift, indicating *c.* 110 m of uplift since OIS 22. This is, first, because the Struma is a significantly larger river and so likely to be better able to incise fully in response to regional uplift and, second, because of the absence of slip on the normal faults bounding the Sandanski Basin since *c.* 4 Ma.

To constrain the less well-resolved earlier part of the uplift history, additional data points are added. The first comes from the pediment of 'Eopleistocene' (i.e. Early Pleistocene) gravel that seals the West Pirin normal fault above Ilindentsi (see above). At this fault, this tributary gravel is at *c.* 940 m a.s.l., but it descends towards the Struma at a gradient of *c.* 4°, reaching as low as *c.* 500 m a.s.l. (*c.* 300 m above present river level) (Zagorchev 1992*a*). Zagorchev (1995) also reported lower pediments inset into it, at *c.* 480–400, 360–320 and *c.* 270–220 m a.s.l. The last of these presumably grades into one of the youngest Struma terraces and the third into the terrace level that has been assigned to OIS 22 (Table 1) (see Galabov 1982; Zagorchev 1992*a*). However, the *c.* 400 m pediment provides a second additional data point, indicating *c.* 200 m of incision. Next, it was estimated above that near the active Krupnik normal fault the Struma has incised since 3 Ma at a time-averaged rate of *c.* 0.08 mm a^{-1} in the hanging wall and that the lower bound to the footwall incision rate has been *c.* 0.18 mm a^{-1}. The average of these two values, *c.* 0.13 mm a^{-1}, is taken as representative of the component of regional uplift, implying *c.* 400 m of uplift since 3 Ma. It is clear that this is a very crude calculation, but nothing better seems possible at this stage given the extent of uncertainty regarding the incision history of this footwall (discussed earlier). Finally, the average altitude, between footwall and hanging-wall cutoffs, of the top of the Sandanski Formation at Melnik is *c.* 500 m (see above). Local evidence (the brackish-water sedimentation in close proximity to the marine sedimentation in the Serrai Graben in the Meiotian, when these two depocentres were evidently interconnected; see above) indicates that this sediment was deposited near sea level. Allowing for possible net glacioeustatic sea-level fall, *c.* 450 m of net uplift can thus be estimated since *c.* 7 Ma. This is broadly consistent with the estimate from the Kresna gorge, also suggesting that regional uplift was slow between *c.* 7 and *c.*

Table 1. Altitudes of Struma and Mesta river terraces

Terrace	Nominal age	Struma altitude (m)	Mesta altitude (m)	Nominal altitude (m)	Preferred OIS
T1	Late Pleistocene	5–7	8–12	6	2
T2	Late Pleistocene	8–12	18–24	10	4
T3	Mid-Pleistocene	20–22	28–30	21	6
T4	Mid-Pleistocene	40–45	40–45	40	8
T5	Early Pleistocene	60–65	60	63	12
T6	Early Pleistocene	85–100	80–90	90	16
T7	Eopleistocene	–	100–110	110	22

Terrace altitude data (above present river level) are from the compilation by Zagorchev (1995), based on Nenov *et al.* (1972) and Galabov (1982). Previously assigned terrace 'ages' use the Russian definition of the Pleistocene. In this scheme, the Eopleistocene is equivalent to the international Early Pleistocene (i.e. from *c.* 1.8 Ma to *c.* 780 ka or OIS 19), the Early Pleistocene is equivalent to the international early Mid-Pleistocene (i.e. to OIS 12), and the Mid-Pleistocene is equivalent to the international late Mid-Pleistocene (i.e. to OIS 6). Nominal altitude means the altitude considered representative for each terrace, used in the uplift modelling in Figure 13. Preferred OIS is the preferred oxygen isotope stage to which each terrace is assigned as a result of this modelling.

3 Ma. The high degree of erosion since the Late Miocene–Early Pliocene and the resulting obliteration of so much former sedimentary evidence clearly makes it difficult to estimate precise amounts of incision, and thus uplift, on this time scale. This is another point of similarity to recent investigations of this topic in western Turkey (see Westaway *et al.* 2004).

The possibility was also considered of using the *c.* 600 m a.s.l. present-day altitude of the Oligocene shallow marine sediment in the Padezh Basin (Fig. 2) as an uplift constraint. However, the strong tilt of these sediments makes it difficult to select any particular altitude datum for them. None the less, these sediments do suggest much slower uplift rates during the Miocene than since, consistent with the evidence from the Sandanski Basin. Their low altitudes also preclude the idea, held by some workers, that before its extension the Aegean region was a high plateau analogous to modern Tibet.

To constrain the associated uplift history, these data are modelled using the technique of Westaway (2001) (see also Westaway *et al.* 2002). This calculates the isostatic response to forcing of lower-crustal flow by cyclic loading at the Earth's surface. It is used here to model, as an approximation, an isostatic uplift response that is probably mainly the result instead of variations in erosion rates; but, as noted by Westaway (2002*b*), these two distinct processes can induce very similar uplift responses.

The results (Fig. 13) can be compared with modelled uplift histories for western Turkey, such as Westaway *et al.* (2004, fig. 21). The total uplift of *c.* 400 m estimated since the Early Pliocene is similar in both regions. However, in western Turkey this seems to be partitioned with *c.* 150 m of uplift since the late Early Pleistocene and *c.* 200–250 m of uplift during the Late Pliocene and early Early Pleistocene. In SW Bulgaria, the proportion during the later of these two phases is lower, *c.* 110 m, and that in the earlier phase correspondingly higher.

A priori, faster erosion was expected in SW Bulgaria than in western Turkey, as the former has been more severely glaciated during cold stages of the Pleistocene (see Demir *et al.* 2004). The modern profuse vegetation in SW Bulgaria, which is expected to inhibit erosion of the unlithified Late Cenozoic sediments, will of course have died back during cold stages. The lower uplift rates estimated for the Mid–Late Pleistocene thus at first sight appear surprising. This modelling indeed suggests substantial erosion rates; for instance, the Sandanski Basin has been incised by *c.* 300 m since *c.* 2 Ma at a time-averaged rate of *c.* 0.15 mm a^{-1}, whereas the spatial average erosion rate for western Turkey seems to be *c.* 0.1 mm a^{-1} (see Westaway 1994; Westaway *et al.* 2004). However, only a small proportion of the present study region in SW Bulgaria, perhaps *c.* 20%, is occupied by eroding Late Cenozoic sedimentary basins (Fig. 2), whereas the proportion is rather higher in western Turkey (see Westaway *et al.* 2004). It can thus be inferred that the overall spatial average erosion rate for SW Bulgaria, calculated as a weighted average of *c.* 0.15 mm a^{-1} for the basins and a rather lower value for the mountain massifs, is less than the *c.* 0.1 mm a^{-1} spatial average value for western Turkey; hence the lower uplift rates in the Mid–Late Pleistocene.

The *c.* 3 Ma start of this initial phase of uplift is considered to reflect global climate change and to thus have no connection with the *c.* 4 Ma

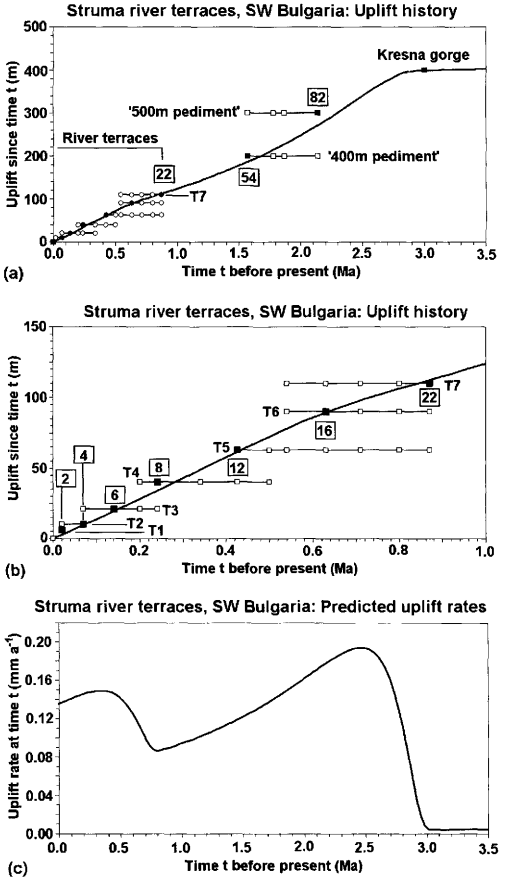

Fig. 13. Uplift histories for the Struma in and around the Sandanski Basin, matched to the observational evidence from river terraces, pediments and gorge incision. Calculations follow the method of Westaway (2001) and Westaway *et al.* (2002), and are based on the following parameter values (defined in these references): z_b 15 km; z_i 27 km; c 20°C km^{-1}; κ 1.2 mm^2 s^{-1}; $t_{o,1}$ 18 Ma, $\Delta T_{c,1}$ −10°C; $t_{0,2}$ 3.1 Ma, $\Delta T_{c,2}$ −15.3°C; $t_{o,3}$ 0.9 Ma, $\Delta T_{c,3}$ −6.5°C. (**a**) Predicted uplift history and supporting data for the Pliocene and Quaternary; (**b**) enlargement of (**a**) showing the late Early Pleistocene onwards; (**c**) predicted variation in uplift rates for the same time scale as in (**a**). Solution predicts 112 m of uplift since 870 ka (OIS 22), 119 m since OIS 25, and 400 m since 3.1 Ma. Peak uplift rates are 0.194 mm a^{-1} at 2.45 Ma and 0.149 mm a^{-1} at 0.35 Ma.

reorganization of Aegean kinematics. However, the relative timing of these two events is not well constrained. None the less, the evidence suggests that the incision post-dates the kinematic reorganization, implying that sedimentation continued in the Sandanski Basin and elsewhere after slip ceased on the bounding normal faults (as shown schematically in Fig. 11). This is consistent, for instance, with the deduction that the uppermost Kalimantsi Formation post-dates the end of slip on the Gorno Spanchevo fault (Fig. 10c and d).

The possible role of low-angle normal faulting

The possibility of large-scale extension in SW Bulgaria before or during the Late Miocene, on normal faults that formed at dips of *c.* 30° or less and took up tens of kilometres of extension, exhuming the mountain ranges in their footwalls from mid-crustal depths as metamorphic core complexes, has been debated. On the one hand, studies such as those by Dinter & Royden (1993), Dinter *et al.* (1995), Shipkova & Ivanov (1999, 2000, 2001) and Burchfiel *et al.* (2000, 2003) have argued this, based on diverse structural and thermochronological evidence. On the other hand, their claims have been repeatedly disputed, notably by Zagorchev (1994, 1998*a*, 2001*b*).

Part of this dispute relates to granites. Zagorchev (1995, 1998*a*,*b*) has distinguished three characteristic granite intrusion ages in SW Bulgaria: Hercynian, Late Cretaceous (*c.* 90 Ma), and Oligocene (*c.* 35 Ma), each with distinct geochemical, petrological and structural characteristics (for instance, the ones considered younger show less evidence of deformation), supported by isotopic dating (Fig. 7). However, others (e.g. Dinter & Royden 1993; Dinter *et al.* 1995) have argued that intrusion of all these granites was synkinematic with large-scale Oligocene or Miocene crustal extension. In such a view, the presence of Hercynian or Cretaceous zircons in some granites can be explained by reworking of this stable mineral into Cenozoic magmas. Exactly the same disputes have occupied the recent literature on western Turkey: whether ancient zircons are *in situ* or reworked (see Loos & Reischmann 1999, 2001); whether Ar–Ar dates for minerals with low closure temperatures in granite plutons indicate intrusion ages or cooling ages (see Westaway 1996, 2005); and whether such cooling was caused simply by erosion or by 'tectonic denudation' by low-angle normal faulting (see Hetzel *et al.* 1995; Lips *et al.* 2001; Ring *et al.* 2003; Westaway 2006). My own recent modelling (Westaway 2006) suggests that the available thermochronologic dataset for western Turkey can be well explained as a result of perturbations to the geothermal gradient caused by erosion and by past changes to the geometry of subduction. However, although such results are consistent with the available evidence, they cannot be proven: one has no way of knowing

what rates of erosion or geometries of subduction were in the Early–Mid-Cenozoic; one can only make estimates, for input into numerical models.

The arguments by Shipkova & Ivanov (1999, 2000, 2001), that Late Cenozoic low-angle normal faulting on their 'Dzherman detachment' was synkinematic with intrusion of the Kalin pluton, depend entirely on the assumption that this normal fault zone is analogous to others where this combination of processes has been claimed (e.g. by Dinter & Royden 1993; Dinter *et al.* 1995) to have occurred; no new evidence has been offered. Their arguments seem in my view to not be worth considering further (see Zagorchev 2001*b*). The papers by Dinter & Royden (1993), Dinter *et al.* (1995) and Burchfiel *et al.* (2000) initially developed the idea of low-angle normal faulting from evidence in Greece, and then applied this idea to SW Bulgaria. Of the two sites in the Sandanski Basin considered by Burchfiel *et al.* (2000) to reflect low-angle normal faulting, at one (Ilindentsi) their interpretation is clearly wrong, being based on a mistake regarding the local geology (Fig. 10a). The second, the Gorno Spanchevo Fault, is clearly steep for much of its length (see above, also Fig. 9). Moreover, given the standard vertical shear construction (Westaway & Kusznir 1993), the *c.* 25° tilting of the oldest sediments in the Sandanski Basin means that fault surfaces with present-day dips of 30°, 40° or 50° would restore, respectively, to 46°, 53° or 59°, plausible initial dips of a conventional steep normal fault. The roadcut site at Gorno Spanchevo (Fig. 10c and d) is admittedly problematic, but it does seem inappropriate for Burchfiel *et al.* (2000) to have emphasized the apparent low-angle fault dip inferred at this one site rather than the preponderance of other evidence that contradicts the inference of such a low-angle dip.

Arguably the most compelling reasoning for low-angle normal faulting in the present study region comes from the analysis by Dinter *et al.* (1995) of the cooling history of the Symvolon pluton near Kavala (see Kyriakopoulos *et al.* 1996; Fig. 1a). They regarded this cooling as accompanying large-scale SW extension on a low-angle normal fault, their 'Strymon detachment', which they inferred as synkinematic with the Gorno Spanchevo Fault. Those workers deduced rapid cooling of this inferred footwall from *c.* 750°C to *c.* 150°C during *c.* 25–15 Ma from U–Pb dating of zircon and titanite and Ar–Ar dating of hornblende, biotite and K-feldspar. However, their dates for zircon (closure temperature T_c 750°C) of *c.* 25 Ma depend on the isotope ratio analysed; one sample yielded a $^{206}Pb/^{238}U$ age as low as 24.4 ± 0.7 Ma but several yielded $^{207}Pb/^{206}Pb$ ages of up to *c.* 300 Ma, consistent with a Hercynian intrusion age (see Kokkinakis 1980; Zagorchev, 1998*a*). The U–Pb dating of titanite includes even greater systematic errors between numerical ages from different isotope ratios. Furthermore, K-feldspar has complex closure behaviour as a result of its complex microstructure; the T_c of 150°C adopted by Dinter *et al.* (1995) is a lower bound that is appropriate only for very slow cooling (see McDougall & Harrison 1999). If one removes the data for these three isotopic systems one is left with a dataset indicating cooling from *c.* 500°C at *c.* 20 Ma (Ar closure in hornblende) to *c.* 350°C at *c.* 15 Ma (Ar closure in biotite). This cooling history closely resembles what is observed (in datasets by Hetzel *et al.* 1995; Lips *et al.* 2001; Ring *et al.* 2003) for the central Menderes Massif in western Turkey (between the Alaşehir and Büyük Menderes grabens; Fig. 1a). Such a cooling history can be explained as a consequence of exhumation by erosion while the region was simultaneously being cooled from below by incipient subduction at a low angle (Westaway 2006), thus removing any basis for inferring low-angle normal faulting in the first place.

Recent studies (e.g. Kounov *et al.* 2001, 2004; Burchfiel *et al.* 2003) have begun to focus on the possibility of large-scale Palaeogene (Eocene–Oligocene) extension by low-angle normal faulting in SW Bulgaria. This is in accordance with a recent trend in western Turkey, whereby researchers (e.g. Purvis & Robertson 2004) have accepted that the Late Cenozoic extension occurred on initially steep normal faults, but have allowed the possibility of a different geometry of normal faulting at an earlier stage. Kounov *et al.* (2001) suggested from thermochronological data that the Osogovo Mountains (Fig. 2) experienced Palaeogene extension by low-angle normal faulting. However, their own data have no simple interpretation in terms of this process. In the 'conventional' geological literature, these mountains are interpreted (see Zagorchev 1995, 2001*a*) as having been intruded by Hercynian granite, then overthrust probably in the Late Cretaceous, then subjected to prolonged erosion. Burchfiel *et al.* (2003) argued for a phase of Eocene to Early Oligocene ENE–WSW extension on their 'Mesta Detachment', which they regarded as contemporaneous with their inferred extension across the Padezh Basin (see above) and the Oligocene extrusive volcanism in the Mesta Basin (Fig. 7). However, the supporting evidence that they presented was rather limited; it amounts to another claim that angular breccia marks a low-angle normal fault rather than possibly indicating slope processes (see Shipkova & Ivanov 1999,

2000, 2001; see above), and an assertion that tilting of beds must be due to extension, when local literature (e.g. Zagorchev 1992*a*) includes multiple phases of deformation in different senses, which could have caused this tilting. As this literature already includes a range of possible interpretations of the Palaeogene evolution of this area (see Zagorchev 1992*a*, 1998*b*, 2001*a*), it would seem more productive to begin further investigation of this topic by testing these existing hypotheses rather than proposing entirely new ones on the basis of limited evidence.

Conclusions

Since the Early Pliocene (*c.* 4 Ma), SW Bulgaria has accommodated southward or SSE extension at several millimetres per year, superimposed on *c.* 400 m of post-Early Pliocene regional uplift. This sense of deformation superseded earlier extension, oriented ENE–WSW, which is estimated to have begun in the early Late Miocene (*c.* 10–9 Ma) and lasted until *c.* 4 Ma, the regional topography being dominated by NNW–SSE-striking normal fault escarpments and grabens that are relics from this time. Normal faults that are now active cut across these older structures, although in some localities normal faults that were oriented obliquely to the earlier extension have remained active, also oblique to the modern extension sense. It is suggested that this present phase of extension relates to the modern sense of deformation throughout the Aegean region and to the modern geometry of the NAFZ, which is independently inferred to have existed since *c.* 4 Ma. The earlier ENE–WSW extension is inferred to have involved two phases, the first pre-dating the NAFZ and the second synkinematic with its initial phase of slip during *c.* 7–4 Ma, when its geometry and the overall sense of deformation throughout the Aegean region were different from at present. Some previous studies have inferred that SW Bulgaria experienced large-scale extension on low-angle normal faults in the Mid-Miocene or earlier. However, the limited evidence in support of this view is open to other interpretations, and after due consideration can be discounted.

I thank I. Zagorchev and R. Nakov for helpful discussions and guidance in the field, and M. Coltorti and M. Tranos for thoughtful and constructive reviews. This study contributes to IGCP 449 'Global correlation of Late Cenozoic fluvial sequences' and to IGCP 518 'Fluvial sequences as evidence for landscape and climatic evolution in the Late Cenozoic'.

References

ALLEN, M., JACKSON, J. & WALKER, R. 2004*a*. Late Cenozoic reorganization of the Arabia–Eurasia collision and the comparison of short-term and long-term deformation rates. *Tectonics*, **23**(1), TC2008, doi 10.1029/2003TC001530.

ALLEN, M., JACKSON, J. & WALKER, R. 2004*b*. Reply to comment by R. Westaway on 'Late Cenozoic reorganization of the Arabia–Eurasia collision and the comparison of short-term and long-term deformation rates' by M. Allen, J. Jackson, & R. Walker. *Tectonics*, **23**(5), TC5007, doi 10.1029/2004TC001695.

AMBRASEYS, N. N. 2001. The Kresna earthquake of 1904 in Bulgaria. *Annali de Geofisica*, **44**, 95–117.

ANDREWS, P., HARRISON, T., DELSON, E., BERNOR, R.L. & MARTIN, L. 1996. Distribution and biochronology of European and southwest Asian Miocene catarrhines. *In*: BERNOR, R. L., FAHLBUSCH, V. & MITTMANN, H.-W. (eds) *The Evolution of Western Eurasian Neogene Mammal Faunas*. Columbia University Press, New York, 168–207.

ARMIJO, R., MEYER, B., HUBERT, A. & BARKA, A. 1999. Westward propagation of the North Anatolian fault into the northern Aegean: timing and kinematics. *Geology*, **27**, 267–270.

ATHANASSIOU, A. & KOSTOPOULOS, D. S. 2001. Proboscidea of the Greek Pliocene–Early Pleistocene faunas: biochronological and palaeoecological implications. *In*: CAVARETTA, G., GIOIA, P., MUSSI, M. & PALOMBO, M. R. (eds) *The World of Elephants: Proceedings of the 1st International Congress, Rome, 16–20 October 2001*. Consiglio Nazionale delle Ricerche, Rome, 85–90.

BERNOR, R. L., KOUFOS, G. D., WOODBURNE, M. O. & FORTELIUS, M. 1996. The evolutionary history and biochronology of the European and Southwest Asian Late Miocene and Pliocene hipparionine horses. *In*: BERNOR, R. L., FAHLBUSCH, V. & MITTMANN, H.-W. (eds) *The Evolution of Western Eurasian Neogene Mammal Faunas*. Columbia University Press, New York, 307–338.

BONCHEV, G. 1912. Prinos kum petrografyata i mineralogyata na Rila Planina. *Spisanie na Bulgarska Academiya na Naukite*, **2**, 1–176.

BOTEV, E., DIMITROV, D. & GEORGIEV, I. 2001. Principal tectonic stress tensor in the region of the Kroupnik Fault from seismic and geodetic data. *Geologica Balcanica*, **31**, 92–93.

BOZKURT, E. 2000. Timing of extension on the Büyük Menderes Graben, western Turkey, and its tectonic implications. *In*: BOZKURT, E., WINCHESTER, J. A. & PIPER, J. D. A. (eds) *Tectonics and Magmatism of Turkey and the Surrounding Area*. Geological Society, London, Special Publications, **173**, 385–403.

BUNBURY, J. M., HALL, L., ANDERSON, G. J. & STANNARD, A. 2001. The determination of fault movement history from the interaction of local drainage with volcanic episodes. *Geological Magazine*, **138**, 185–192.

BURCHFIEL, B. C., NAKOV, R., TZANKOV, T. & ROYDEN, L. H. 2000. Cenozoic extension in Bulgaria and northern Greece; the northern part of

the Aegean extensional regime. *In*: BOZKURT, E., WINCHESTER, J. A. & PIPER, J. D. A. (eds) *Tectonics and Magmatism in Turkey and the Surrounding Area*. Geological Society, London, Special Publications, **173**, 325–352.

BURCHFIEL, C. B., NAKOV, R. & TZANKOV, T. 2003. Evidence from the Mesta half-graben, SW Bulgaria, for the Late Eocene beginning of Aegean extension in Central Balkan Peninsula. *Tectonophysics*, **375**, 61–76.

DEMİR, T., YEŞİLNACAR, İ. & WESTAWAY, R. 2004. River terrace sequences in Turkey: sources of evidence for lateral variations in regional uplift. *Proceedings of the Geologists' Association*, **115**, 289–311.

DINTER, D. & ROYDEN, L. 1993. Late Cenozoic extension in north-eastern Greece: Strymon valley detachment system and Rhodope metamorphic core complex. *Geology*, **21**, 45–48.

DINTER, D., MACFARLANE, A., HAMES, W., ISACHSEN, C., BOWRING, C. & ROYDEN, L. 1995. U–Pb and $^{40}Ar/^{39}Ar$ geochronology of the Symvolon granodiorite: implications for the thermal and structural evolution of the Rhodope metamorphic core complex, north-eastern Greece. *Tectonics*, **14**, 886–908.

ERİNÇ, S. 1978. Changes in the physical environment in Turkey since the end of the last glacial. *In*: BRICE, W. C. (ed.) *The Environmental History of the Near and Middle East since the Last Ice Age*. Academic Press, London, 87–110.

FURLAN, D. 1977. The climate of southeast Europe. *In*: WALLEN, C. C. (ed.) *Climates of Central and Southern Europe. World Survey of Climatology, Volume 6*. Elsevier, Amsterdam, 185–235.

GALABOV, Z. 1982. *Geography of Bulgaria. Physical Geography*. Bulgarian Academy of Sciences, Sofia.

GENTRY, A. W. & HEIZMANN, E. P. J. 1996. Miocene ruminants of the central and eastern Tethys and Paratethys. *In*: BERNOR, R. L., FAHLBUSCH, V. & MITTMANN, H.-W. (eds) *The Evolution of Western Eurasian Neogene Mammal Faunas*. Columbia University Press, New York, 378–391.

GERAADS, D., SPASSOV, N. & KOVACHEV, D. 2001. New Chalicotheriidae (Perissodactyla, Mammalia) from the Late Miocene of Bulgaria. *Journal of Vertebrate Paleontology*, **21**, 596–606.

GRAMMAN, F. & KOCKEL, F. 1969. Das Neogen im Strimonbecken (Griechisch–Ostmazedonien)—1, Lithologie, Stratigraphie und Paläogeographie. *Geologisches Jahrbuch*, **87**, 445–484.

HEISSIG, K. 1996. The stratigraphical range of fossil rhinoceroses in the Late Neogene of Europe and the Eastern Mediterranean. *In*: BERNOR, R. L., FAHLBUSCH, V. & MITTMANN, H.-W. (eds) *The Evolution of Western Eurasian Neogene Mammal Faunas*. Columbia University Press, New York, 339–347.

HETZEL, R., RING, U., AKAL, C. & TROESCH, M. 1995. Miocene NNE-directed extensional unroofing in the Menderes Massif, southwestern Turkey. *Journal of the Geological Society, London*, **152**, 639–654.

HUBERT-FERRARI, A., ARMIJO, R., KING, G., MEYER, B. & BARKA, A. 2002. Morphology, displacement, and slip rates along the North Anatolian Fault, Turkey. *Journal of Geophysical Research*, **107**(B10), JB2235, doi: 10.1029/2001JB000393.

IVANOV, D. 1995. Palynological data on fossil flora from the village of Ognjanovo (southwestern Bulgaria). *Phytologia Balcanica*, **2**, 3–14.

JACKSON, J. A. & MCKENZIE, D. P. 1988. Rates of active deformation in the Aegean Sea and surrounding regions. *Basin Research*, **1**, 121–128.

JACKSON, J. A., KING, G. C. P. & VITA-FINZI, C. 1982. The neotectonics of the Aegean: an alternative view. *Earth and Planetary Science Letters*, **61**, 303–318.

KAMENOV, B. & KOJUMDGIEVA, E. 1983. Stratigraphy of the Neogene of Sofia Basin. *Palaeontologiya, Stratigrafiya i Lithologiya*, **18**, 69–85 (in Bulgarian with English summary).

KARISTINEOS, N. K. & GEORGIADES-DIKEOULIA, E. 1986. The marine transgression in the Serres Basin. *Annales Géologiques des Pays Helleniques*, **33**, 221–232.

KISSEL, C. & LAJ, C. 1988. The Tertiary geodynamical evolution of the Aegean arc: a palaeomagnetic reconstruction. *Tectonophysics*, **146**, 183–201.

KOÇYİĞİT, A., YUSUFOĞLU, H. & BOZKURT, E. 1999. Evidence from the Gediz graben for episodic two-stage extension in western Turkey. *Journal of the Geological Society, London*, **156**, 605–616.

KOJUMDGIEVA, E., NIKOLOV, I., NEDJALKOV, P. & BUSEV, A. 1982. Stratigraphy of the Neogene in Sandanski Graben. *Geologica Balcanica*, **12**, 69–81.

KOKKINAKIS, A. 1980. Altersbeziehungen zwischen Metamorphosen, mechanischen Deformationen und Intrusionen am Südrand des Rhodope-Massivs (Makedonien, Griechenland). *Geologische Rundschau*, **69**, 726–744.

KONYAROV, G. 1932. *Kafyavite vuglisha v Bulgaria*. Durzhavni Mili, Pernik.

KOTZEV, V., NAKOV, R., BURCHFIEL, B. C., KING, R. & REILINGER, R. 2001. GPS study of active tectonics in Bulgaria; results from 1996 to 1998. *Journal of Geodynamics*, **31**, 189–200.

KOUNOV, A., SEWARD, D., BERNOULLI, D., BURG, J.-P. & IVANOV, Z. 2001. Timing of Cenozoic extension in the Kraishte region (SW Bulgaria): evidence from fission track analysis. *Geologica Balcanica*, **31**, 112–113.

KOUNOV, A., SEWARD, D., BERNOUILLI, D., BURG, J.-P. & IVANOV, Z. 2004. Thermotectonic evolution of an extensional dome; the Cenozoic Osogovo–Lisets core complex; Kraishte Zone, Western Bulgaria. *International Journal of Earth Sciences*, **93**, 1008–1024.

KUKLA, G. J. 1975. Loess stratigraphy of central Europe. *In*: BUTZER, K. W. & ISAAC, G. L. (eds) *After the Australopithecines*. Mouton, The Hague, 99–188.

KUKLA, G. J., 1978. The classical European glacial stages: correlation with deep-sea sediments. *Transactions of the Nebraska Academy of Sciences*, **6**, 57–93.

KYRIAKOPOULOS, K., MAGGANAS, A., NORELLI, O., BIGAZZI, G., DEL MORO, A. & KOKKINAKIS, A. 1996. Thermochronological evolution of Symvolon and Pangeon plutons and their country rocks, Kavala area, N. Greece: an apatite fission track

analysis. *Neues Jahrbuch für Mineralogie, Monatshefte*, **1996**(11), 519–529.

LIPS, A. L. W., CASSARD, D., SÖZBİLİR, H., YILMAZ, H. & WIJBRANS, J. R. 2001. Multistage exhumation of the Menderes Massif, western Anatolia (Turkey). *International Journal of Earth Sciences*, **89**, 781–792.

LOOS, S. & REISCHMANN, T. 1999. The evolution of the southern Menderes Massif in SW Turkey as revealed by zircon dating. *Journal of the Geological Society, London*, **156**, 1021–1030.

LOOS, S. & REISCHMANN, T. 2001. Reply to comment by Bozkurt, E. and Park, R.G., on 'The evolution of the southern Menderes Massif in SW Turkey as revealed by zircon dating'. *Journal of the Geological Society, London*, **158**, 394–395.

LUNGU, A. & OBADA, T. 2001. Contributions to the study of the Neogene representatives of ordo Proboscidea (Mammalia) from eastern Europe. *In*: CAVARETTA, G., GIOIA, P., MUSSI, M. & PALOMBO, M. R. (eds) *The World of Elephants: Proceedings of the 1st International Congress, Rome, 16–20 October 2001*. Consiglio Nazionale delle Ricerche, Rome, 119–121.

MARINOVA, R. 1991. *Geological Map of the People's Republic of Bulgaria, 1:100 000 series, Blagoevgrad sheet*. Geological Institute, Bulgarian Academy of Sciences, Sofia.

MARINOVA, R. & ZAGORCHEV, I. 1990. *Geological Map of the People's Republic of Bulgaria, 1:100 000 series, Razlog sheet*. Geological Institute, Bulgarian Academy of Sciences, Sofia.

MCCLUSKY, S., BALASSANIAN, S., BARKA, A., *et al.* 2000. Global Positioning System constraints on plate kinematics and dynamics in the eastern Mediterranean and Caucasus. *Journal of Geophysical Research*, **105**, 5695–5719.

MCDOUGALL, I. & HARRISON, T. M. 1999. *Geochronology and Thermochronology by the $^{40}Ar/^{39}Ar$ Method*, 2nd ed. Oxford University Press, Oxford.

MCKENZIE, D. & JACKSON, J. 1983. The relationship between strain rates, crustal thickening, palaeomagnetism, finite strain and fault movements within a deforming zone. *Earth and Planetary Science Letters*, **65**, 182–202.

MEIJER, P. T. & WORTEL, M. J. R. 1997. Present-day dynamics of the Aegean region: a model analysis of the horizontal pattern of stress and deformation. *Tectonics*, **16**, 879–895.

MEYER, B., ARMIJO, R. & DIMITROV, D. 2002. Active faulting in SW Bulgaria; possible surface rupture of the 1904 Struma earthquakes. *Geophysical Journal International*, **148**, 246–255.

MOSKOVSKI, S. 1983. Certains particularités des sediments paléogènes et plio-pléistocènes dans les parties moyennes de la vallée de Struma. *Réunion Extraordinaire de la Société Géologique de France, Guide de l'Excursion*, 105–108.

MUDELSEE, M. & SCHULZ, M. 1997. The Mid-Pleistocene climate transition: onset of 100 ka cycle lags ice volume build-up by 280 ka. *Earth and Planetary Science Letters*, **151**, 117–123.

NEDJALKOV, P., TCHEREMISIN, N., KODUMDGIEVA, E., TZATZEV, B. & BUZEV, A. 1986. Facial and paleogeographic features of Neogene deposits in the Sandanski graben. *Geologica Balcanica*, **18**, 61–66.

NENOV, T., SLAVOV, I. & STOYKOV, S. 1972. Pliocene and Quaternary in the Gotse Delchev depression and principal stages in its neotectonic development. *Review of the Bulgarian Geological Society*, **33**, 195–203 (in Bulgarian with English summary).

NIKOLOV, I. 1985. Catalogue of the localities of Tertiary mammals in Bulgaria. *Palaeontologiya, Stratigrafiya i Lithologiya*, **21**, 43–61 (in Bulgarian with English summary).

OGNJANOVA, N. & YANEVA, M. 2001. New data about Baldevo Formation, Gotse Delchev Basin, based on sedimentological and biostratigraphical evidences. *Geologica Balcanica*, **31**, 127–128.

OKAY, A. I., TÜYSÜZ, O. & KAYA, Ş. 2004. From transpression to transtension: changes in morphology and structure around a bend on the North Anatolian Fault in the Marmara region. *Tectonophysics*, **291**, 259–282.

PALMAREV, E. 1970. Fossile floren aus drei Braunkohlenbecken in Südwestbulgarien. *Izvesti na Botanicheskiya Institut Bulgarska Academiya na Naukite*, **20**, 35–79 (in Bulgarian with German abstract).

PALMAREV, E. 1982. Fosilnata flora na Melnishkiya basein. *Palaeontologiya, Stratigrafiya i Lithologiya*, **16**, 3–44.

PURVIS, M. & ROBERTSON, A. H. F. 2004. A pulsed extension model for the Neogene–Recent E–W trending Alaşehir Graben and the NE–SW trending Selendi and Gördes Basins, western Turkey. *Tectonophysics*, **391**, 171–201.

RICHTER, C. F. 1958. *Elementary Seismology*. Freeman, San Francisco, CA.

RIGO, A., DE CHABALIER, J.-B., MEYER, B. & ARMIJO, R. 2004. The 1995 Kozani–Grevena (northern Greece) earthquake revisited; an improved faulting model from synthetic aperture radar interferometry. *Geophysical Journal International*, **157**, 727–736

RING, U., JOHNSON, C., HETZEL, R. & GESSNER, K. 2003. Tectonic denudation of a Late Cretaceous–Tertiary collisional belt: regionally-symmetric cooling patterns and their relation to extensional faults in the Anatolide Belt of western Turkey. *Geological Magazine*, **140**, 421–441.

ROBERTSON, A. H. F., ÜNLÜGENÇ, U. C., İNAN, N. & TAŞLI, K. 2004. The Misis–Andırın Complex: a Mid-Tertiary mélange related to late-stage subduction of the Southern Neotethys in S Turkey. *Journal of Asian Earth Sciences*, **22**, 413–453.

ROHLING, E. J. & HILGEN, F. J. 1991. The eastern Mediterranean climate at times of sapropel formation: a review. *Geologie en Mijnbouw*, **70**, 253–264.

SEEBER, L., EMRE, O., CORMIER, M.-H., *et al.* 2004. Uplift and subsidence from oblique slip: the Ganos–Marmara bend of the North Anatolian transform, western Turkey. *Tectonophysics*, **391**, 239–258.

SEYİTOĞLU, G. & SCOTT, B. 1992. The age of the Büyük Menderes graben (west Turkey) and its tectonic implications. *Geological Magazine*, **129**, 239–242.

SEYİTOĞLU, G., SCOTT, B. & RUNDLE, C. C. 1992. Timing of Cenozoic extensional tectonics in west

Turkey. *Journal of the Geological Society, London*, **149**, 533–538.

SHACKLETON, N. J., BERGER, A. & PELTIER, W. R. 1990. An alternative astronomical calibration of the lower Pleistocene timescale based on ODP site 677. *Transactions of the Royal Society of Edinburgh, Earth Sciences*, **81**, 251–261.

SHIPKOVA, K. & IVANOV, Z. 1999. The Djerman detachment fault; a result of late Tertiary extension in the north-western parts of the Rhodope Massif, Bulgaria. European Union of Geosciences Conference Abstracts, EUG 10. *Journal of Conference Abstracts*, **4**, 470.

SHIPKOVA, K. & IVANOV, Z. 2000. The Djerman detachment fault; an effect of the late Tertiary extension in the north-west part of the Rhodope Massif. *Dokladi na Bulgarskata Akademia na Naukite*, **53**, 81–84.

SHIPKOVA, K. & IVANOV, Z. 2001. Effects of Late Alpine extension in the northwestern foot of Rila Mountain. *Geologica Balcanica*, **31**, 138–139.

SOUFLERIS, C., JACKSON, J. A., KING, G. C. P., SPENCER, C. P. & SCHOLZ, C. H. 1982. The 1978 earthquake sequence near Thessaloniki (northern Greece). *Geophysical Journal of the Royal Astronomical Society*, **68**, 429–458.

STEENBRINK, J., VAN VUGT, N., HILGEN, F. J., WIJBRANS, J. R. & MEULENKAMP, J. E. 1999. Sedimentary cycles and volcanic ash beds in the lower Pliocene lacustrine succession of Ptolemais (NW Greece); discrepancy between $^{40}Ar/^{39}Ar$ and astronomical ages. *Palaeogeography, Palaeoclimatology, Palaeoecology*, **152**, 283–303.

STEENBRINK, J., VAN VUGT, N., KLOOSTERBOER-VAN HOEVE, M. L. & HILGEN, F. J. 2000. Refinement of the Messinian APTS from sedimentary cycle patterns in the lacustrine Lava section (Servia Basin, NW Greece). *Earth and Planetary Science Letters*, **181**, 161–173.

STEININGER, F. F., BERGGREN, W. A., KENT, D. V., BERNOR, R. L., SEN, S. & AGUSTI, J. 1996. Circum-Mediterranean Neogene (Miocene and Pliocene) marine–continental chronologic correlations of European mammal units. *In*: BERNOR, R. L., FAHLBUSCH, V. & MITTMANN, H.-W. (eds) *The Evolution of Western Eurasian Neogene Mammal Faunas*. Columbia University Press, New York, 7–46.

TEMNISKOVA, D. & OGNJANOVA, N. 1983. Siliceous algae from fresh-water Neogene diatomites in the Gotse Delchev area. *Fitologiya*, **22**, 29–45 (in Bulgarian with English summary).

TRANOS, M. D., PAPADIMITRIOU, E. E. & KILIAS, A. A. 2003. Thessaloniki–Gerakarou Fault Zone (TGFZ): the western extension of the 1978 Thessaloniki earthquake fault (northern Greece) and seismic hazard assessment. *Journal of Structural Geology*, **25**, 2109–2123.

TÜYSÜZ, O., BARKA, A. & YIĞITBAŞ, E. 1998. Geology of the Saros Graben and its implications fror the evolution of the North Anatolian Fault in the Ganos–Saros region, northwestern Turkey. *Tectonophysics*, **293**, 105–126.

VAN DEN BERG, M. W. & VAN HOOF, T. 2001. The Maas terrace sequence at Maastricht, SE Netherlands: evidence for 200 m of late Neogene and Quaternary surface uplift. *In*: MADDY, D., MACKLIN, M. G. & WOODWARD, J. C. (eds) *River Basin Sediment Systems: Archives of Environmental Change*. Balkema, Rotterdam, 45–86.

VAN VUGT, N., STEENBRINK, J., LANGEREIS, C. G., HILGEN, F. J. & MEULENKAMP, J. E. 1998. Magnetostratigraphy-based astronomical tuning of the early Pliocene lacustrine sediments of Ptolemais (NW Greece) and bed-to-bed correlation with the marine record. *Earth and Planetary Science Letters*, **164**, 535–551.

VAN VUGT, N., LANGEREIS, C. G. & HILGEN, F. J. 2001. Orbital forcing in Pliocene–Pleistocene Mediterranean lacustrine deposits; dominant expression of eccentricity versus precession. *Palaeogeography, Palaeoclimatology, Palaeoecology*, **172**, 193–205.

VASILIEV, I., KRIJGSMAN, W., LANGEREIS, C. G., PANAIOTU, C. E., MATENCO, L. & BERTOTTI, G. 2004. Towards an astrochronological framework for the eastern Paratethys Mio-Pliocene sedimentary sequences of the Focşani Basin (Romania). *Earth and Planetary Science Letters*, **227**, 231–247.

VATSEV, M. 1980. Lithostratigraphy of the Neogene sedimentary rocks of the Gotse Delchev Basin. *Annals of the Higher Institute of Mining and Geology, Sofia*, **25**, 103–115 (in Bulgarian with English summary).

VATSEV, M. & BONEV, P. 1994. Lithostratigraphy of the Neogene from the Kyustendil coal basin. *Reviews of the University of Mining and Geology (St. Ivan Rilski University, Sofia)*, **40**, 43–50.

VELCHEV, A. 1995. Pleistocene glaciation of the Bulgarian Mountains. *Annuaire de l'Université de Sofia, Livre 2, Géographie*, **87**, 53–65.

WESTAWAY, R. 1993. Neogene evolution of the Denizli region of western Turkey. *Journal of Structural Geology*, **15**, 37–53.

WESTAWAY, R. 1994. Evidence for dynamic coupling of surface processes with isostatic compensation in the lower crust during active extension of western Turkey. *Journal of Geophysical Research*, **99**, 20203–20223.

WESTAWAY, R. 1996. Comment on 'Bivergent extension in orogenic belts: the Menderes massif (southwestern Turkey)' by R. Hetzel, C.W. Passchier, U. Ring & Ö.O. Dora. *Geology*, **24**, 93–94.

WESTAWAY, R. 1998. Dependence of active normal fault dips on lower-crustal flow regimes. *Journal of the Geological Society, London*, **155**, 233–253.

WESTAWAY, R. 1999. The mechanical feasibility of low-angle normal faulting. *Tectonophysics*, **308**, 407–443 (Correction: *Tectonophysics*, **341**, 237–238).

WESTAWAY, R. 2001. Flow in the lower continental crust as a mechanism for the Quaternary uplift of the Rhenish Massif, north-west Europe. *In*: MADDY, D., MACKLIN, M. & WOODWARD, J. (eds) *River Basin Sediment Systems: Archives of Environmental Change*. Balkema, Rotterdam, 87–167.

WESTAWAY, R. 2002*a*. Long-term river terrace sequences: evidence for global increases in surface uplift rates in the Late Pliocene and early Middle Pleistocene caused by flow in the lower continental crust induced by surface processes. *Netherlands Journal of Geosciences*, **81**, 305–328.

WESTAWAY, R. 2002*b*. Geomorphological consequences of weak lower continental crust, and its significance for studies of uplift, landscape evolution, and the interpretation of river terrace sequences. *Netherlands Journal of Geosciences*, **81**, 283–304.

WESTAWAY, R. 2002*c*. The Quaternary evolution of the Gulf of Corinth, central Greece: coupling between surface processes and flow in the lower continental crust. *Tectonophysics*, **348**, 269–318.

WESTAWAY, R. 2003. Kinematics of the Middle East and Eastern Mediterranean updated. *Turkish Journal of Earth Sciences*, **12**, 5–46.

WESTAWAY, R. 2004*a*. Kinematic consistency between the Dead Sea Fault Zone and the Neogene and Quaternary left-lateral faulting in SE Turkey. *Tectonophysics*, **391**, 203–237.

WESTAWAY, R. 2004*b*. Comment on 'Late Cenozoic reorganization of the Arabia–Eurasia collision and the comparison of short-term and long-term deformation rates' by M. Allen, J. Jackson, and R. Walker. *Tectonics*, **23**(5), TC5006, doi: 10.1029/2004TC001674.

WESTAWAY, R. 2005. Active low-angle normal faulting in the Woodlark Extensional Province, Papua New Guinea: a physical model. *Tectonics*, **24**, TC6003, doi: 10.1029/2004TC001744.

WESTAWAY, R. 2006. Cenozoic cooling histories in the Menderes Massif, western Turkey, may be caused by erosion and flat subduction, not low-angle normal faulting. *Tectonophysics*, **412**, 1–25.

WESTAWAY, R. & ARGER, J. 1996. The Gölbaşı basin, southeastern Turkey: a complex discontinuity in a major strike-slip fault zone. *Journal of the Geological Society, London*, **153**, 729–743.

WESTAWAY, R. & ARGER, J. 2001. Kinematics of the Malatya–Ovacık fault zone. *Geodinamica Acta*, **14**, 103–131.

WESTAWAY, R. & KUSZNIR, N. J. 1993. Fault and bed 'rotation' during continental extension: block rotation or vertical shear? *Journal of Structural Geology*, **15**, 753–770 (Correction: *Journal of Structural Geology*, **15**, 1391).

WESTAWAY, R., MADDY, D. & BRIDGLAND, D. 2002. Flow in the lower continental crust as a mechanism for the Quaternary uplift of south-east England: constraints from the Thames terrace record. *Quaternary Science Reviews*, **21**, 559–603.

WESTAWAY, R., PRINGLE, M., YURTMEN, S., DEMİR, T., BRIDGLAND, D., ROWBOTHAM, G. & MADDY, D. 2003. Pliocene and Quaternary surface uplift of western Turkey revealed by long-term river terrace sequences. *Current Science*, **84**, 1090–1101.

WESTAWAY, R., PRINGLE, M., YURTMEN, S., DEMİR, T., BRIDGLAND, D., ROWBOTHAM, G. & MADDY, D. 2004. Pliocene and Quaternary regional uplift in western Turkey: the Gediz river terrace staircase and the volcanism at Kula. *Tectonophysics*, **391**, 121–169.

WESTAWAY, R., GUILLOU, H., YURTMEN, S., DEMİR, T. & ROWBOTHAM, G. 2005. Investigation of the conditions at the start of the present phase of crustal extension in western Turkey, from observations in and around the Denizli region. *Geodinamica Acta*, **18**, 313–342.

WESTAWAY, R., DEMİR, T., SEYREK, A. & BECK, A. 2006. Kinematics of active left-lateral faulting in southeast Turkey from offset Pleistocene river gorges: improved constraint on the rate and history of relative motion between the Turkish and Arabian plates. *Journal of the Geological Society, London*, **163**, 149–164.

YALTIRAK, C., SAKINÇ, M. & OKTAY, F. Y. 2000. Comment on 'Westward propagation of the North Anatolian fault into the northern Aegean: timing and kinematics' by Armijo, R., Meyer, B., Hubert, A. & Barka, A. *Geology*, **28**, 187–188.

YILMAZ, Y., GENÇ, S. C., GÜRER, F., *et al*. 2000. When did the Aegean grabens begin to develop? *In*: BOZKURT, E., WINCHESTER, J. A. & PIPER, J. D. A. (eds) *Tectonics and Magmatism in Turkey and the Surrounding Area*. Geological Society, London, Special Publications, **173**, 353–384.

ZAGORCHEV, I. 1992*a*. Neotectonic development of the Struma (Kraištid) lineament, southwest Bulgaria and northern Greece. *Geological Magazine*, **129**, 197–222.

ZAGORCHEV, I. 1992*b*. Neotectonics of the central parts of the Balkan Peninsula: basic features and concepts. *Geologische Rundschau*, **81**, 635–654.

ZAGORCHEV, I. 1994. Comment on 'Late Cenozoic extension in northeastern Greece; Strymon Valley detachment system and Rhodope metamorphic core complex' by Dinter, D.A. and Royden, L. *Geology*, **22**, 283.

ZAGORCHEV, I. 1995. *Pirin; Geological Guidebook*. Professor Martin Drinov Academic Publishing House, Sofia.

ZAGORCHEV, I. 1998*a*. Rhodope controversies. *Episodes*, **21**, 159–166.

ZAGORCHEV, I. 1998*b*. Pre-Priabonian Palaeogene formations in southwestern Bulgaria and northern Greece: stratigraphy and tectonic implications. *Geological Magazine*, **135**, 101–119.

ZAGORCHEV, I. 2001*a*. Introduction to the geology of SW Bulgaria. *Geologica Balcanica*, **31**, 3–52.

ZAGORCHEV, I. 2001*b*. Low-angle normal faults and detachment hoaxes in SW Bulgaria. *Geologica Balcanica*, **31**, 142–143.

ZAGORCHEV, I. & DINKOVA, J. 1990. *Geological Map of the People's Republic of Bulgaria, 1:100 000 series, Petrich sheet*. Geological Institute, Bulgarian Academy of Sciences, Sofia.

ZAGORCHEV, I. & MOORBATH, S. 1986. Rb–Sr dating of the granitoid magmatism in Sahtinska Sredna Gora Mountains. *Reviews of the Bulgarian Geological Society*, **47**(3), 62–68 (in Bulgarian with English abstract).

ZAGORCHEV, I., LILOV, P. & MOORBATH, S. 1989*a*. Results of the rubidium–strontium and potassium–argon radiogeochronological studies of the metamorphic and igneous rocks of Southern Bulgaria. *Geologica Balcanica*, **19**, 41–54.

ZAGORCHEV, I., POPOV, N. & RUSEVA, M. 1989*b*. Stratigrafiya Paleogena v chasti yugo-zapadnoi Bulgarii. *Geologica Balcanica*, **19**(6), 41–69.

ZAGORCHEV, I., GORANOV, A., VULKOV, V. & BOYANOV, I. 1999. Palaeogene sediments in the Padala graben, northwestern Rila Mountain, Bulgaria. *Geologica Balcanica*, **29**, 59–69.